Fraunhofer ITWM

W. Arne, N. Marheineke, A. Meister, R. Wegener

Numerical analysis of Cosserat rod and string models for viscous jets in rotational spinning processes

Berichte des Fraunhofer ITWM, Nr. 167 (2009)

ISSN 1434-9973

Bericht 167 (2009)

Die Veröffentlichungen in der Berichtsreihe des Fraunhofer ITWM können bezogen werden über:

Fraunhofer-Institut für Techno- und
Wirtschaftsmathematik ITWM
Fraunhofer-Platz 1

67663 Kaiserslautern
Germany

Telefon: +49(0)631/31600-0
Telefax: +49(0)631/31600-1099
E-Mail: info@itwm.fraunhofer.de
Internet: www.itwm.fraunhofer.de

Vorwort

Das Tätigkeitsfeld des Fraunhofer-Instituts für Techno- und Wirtschaftsmathematik ITWM umfasst anwendungsnahe Grundlagenforschung, angewandte Forschung sowie Beratung und kundenspezifische Lösungen auf allen Gebieten, die für Techno- und Wirtschaftsmathematik bedeutsam sind.

In der Reihe »Berichte des Fraunhofer ITWM« soll die Arbeit des Instituts kontinuierlich einer interessierten Öffentlichkeit in Industrie, Wirtschaft und Wissenschaft vorgestellt werden. Durch die enge Verzahnung mit dem Fachbereich Mathematik der Universität Kaiserslautern sowie durch zahlreiche Kooperationen mit internationalen Institutionen und Hochschulen in den Bereichen Ausbildung und Forschung ist ein großes Potenzial für Forschungsberichte vorhanden. In die Berichtreihe sollen sowohl hervorragende Diplom- und Projektarbeiten und Dissertationen als auch Forschungsberichte der Institutsmitarbeiter und Institutsgäste zu aktuellen Fragen der Techno- und Wirtschaftsmathematik aufgenommen werden.

Darüber hinaus bietet die Reihe ein Forum für die Berichterstattung über die zahlreichen Kooperationsprojekte des Instituts mit Partnern aus Industrie und Wirtschaft.

Berichterstattung heißt hier Dokumentation des Transfers aktueller Ergebnisse aus mathematischer Forschungs- und Entwicklungsarbeit in industrielle Anwendungen und Softwareprodukte – und umgekehrt, denn Probleme der Praxis generieren neue interessante mathematische Fragestellungen.

Prof. Dr. Dieter Prätzel-Wolters
Institutsleiter

Kaiserslautern, im Juni 2001

NUMERICAL ANALYSIS OF COSSERAT ROD AND STRING MODELS FOR VISCOUS JETS IN ROTATIONAL SPINNING PROCESSES

WALTER ARNE, NICOLE MARHEINEKE, ANDREAS MEISTER, AND RAIMUND WEGENER

Abstract. This work deals with the curling behavior of slender viscous jets in rotational spinning processes. In terms of slender-body theory a instationary incompressible viscous Cosserat rod model is formulated which differs from the approach of [17] in the incompressibility approximation and reduces to the string model of [12] for a vanishing slenderness parameter. Focusing exclusively on viscous and rotational effects on the jet in the exit plane near the spinning nozzle, the stationary two-dimensional scenario is described by a two-point boundary value problem of a system of first order ordinary differential equations for jet's center-line, tangent, curvature, velocity, inner shear and traction force and couple. The numerical analysis shows that the rod model covers the string model in an inertia-dominated jet regime. Beyond that it overcomes the limitations of the string model studied in [10] and enables even the handling of the viscous-inertial jet regime. Thus, the rod model shows its applicability for the simulation of industrially relevant parameter ranges and enlarges the domain of validity with respect to the string approach.

Keywords. Rotational spinning process; curved viscous fibers; asymptotic Cosserat models; boundary value problem; existence of numerical solutions
AMS-Classification. 65L10, 76-xx, 41A60

1. Introduction

The rotational spinning of viscous jets is of interest in many industrial applications, including pellet manufacturing [4, 14, 19, 20] and drawing, tapering and spinning of glass and polymer fibers [8, 12, 13], see also [15, 21] and references within. In [12] an asymptotic model for the dynamics of curved viscous inertial fiber jets emerging from a rotating orifice under surface tension and gravity was deduced from the three-dimensional free boundary value problem given by the incompressible Navier-Stokes equations for a Newtonian fluid. In the terminology of [1], it is a string model consisting of balance equations for mass and linear momentum. Accounting for inner viscous transport, surface tension and placing no restrictions on either the motion or the shape of the jet's center-line, it generalizes the previously developed string models for straight [3, 5, 6] and curved center-lines [4, 13, 19]. Moreover, the numerical results investigating the effects of viscosity, surface tension, gravity and rotation on the jet behavior coincide well with the experiments of Wong et.al. [20].

However, the applicability of the string model is restricted to certain parameter ranges. Neglecting surface tension and gravity, already for jets in a stationary, two-dimensional scenario no physically relevant solutions exist for $\mathrm{Rb}^2 < \mathrm{Re}^{-1}$ with Reynolds number $\mathrm{Re}^{-1} \ll 1$ and Rossby number $\mathrm{Rb} \ll 1$, as shown in [10]. The numerical simulations also break down for viscous fiber jets under very high rotations ($\mathrm{Re} \ll 1$, $\mathrm{Rb} \ll 1$) as they occur in industrial production processes of glass wool. When surface tension and gravity are included, the question of existence and solvability becomes even more difficult to answer. Numerical problems are generally encountered at the spinning nozzle for high rotations since huge gradients in the angle arise, [12]. These problems might be handled by modified boundary conditions at the nozzle, see comments and studies to this point in [4, 7, 9, 11]. Alternatively, the incorporation of angular momentum effects and the formulation of a consistent viscous rod theory for rotational spinning raises hope to cover the string model and even more to overcome the restrictions and open the parameter ranges of practical interest to simulation and optimization, in analogy to the previous studies on string and rod models for fluid-mechanical sewing machines in [2, 18]. In that application the coupling of twisting with the motion of the center-line turned out to be crucial for the coiling of a viscous jet falling on a rigid substrate. Ribe

Date: July 6, 2009.

proposed the underlying viscous rod model that allows for stretching, bending and twisting. Its asymptotic derivation was based on the cross-sectional averaging of the balance laws for mass, linear and and angular momentum. The assumptions of a stationary and moderately curved center-line in [16] were released in [17] to describe a dynamic center-line.

In this work, we develop an incompressible viscous Cosserat rod model for rotational spinning processes and compare it theoretically and numerically with the string model in view of performance, validity and applicability. Enabling the simulation of practically relevant parameter ranges and particularly the investigation of the curling behavior of the fiber jet near the spinning nozzle, the rod model shows its expected superiority to the string model. However, the simpler string model turns out to a good approximation to the rod model in an inertia-dominated jet regime for high Reynolds number flows. In case of negligible thickness, the models even coincide.

This paper is structured as follows. Starting with a short introduction into the specific Cosserat rod theory according to [1], we develop an instationary viscous rod model in a Lagrangian framework based on an incompressible geometrical model and appropriate constitutive laws in section 2. Moreover, we discuss its difference to Ribe's proposed rod model [17] in an Eulerian setting (see (2.8) for our Cosserat model). In section 3, we apply the rod model to rotational spinning of slender, viscous jets. Focusing on the curling behavior the jet near the nozzle in dependence of viscous friction Re and rotation Rb, we consider a simplified, stationary two-dimensional scenario. We come up with a two-point boundary value problem of first order ordinary differential equations (3.4) for jet's center-line, tangent, curvature, velocity, inner shear and traction force and couple, whose limit for a vanishing slenderness parameter ϵ corresponds to the string model of [13, 12]. Providing an appropriate numerical method, we proceed with the numerical analysis of rod and string model and compare the results in view of performance and applicability. Two jet regimes, i.e. inertial and viscous-inertial regime, arise in rotational spinning – dependently on the considered parameters $(\mathrm{Re}, \mathrm{Rb}, \epsilon)$ –, which we investigate numerically in section 4. We finally conclude with jet simulations for parameter ranges of practical interest.

2. Cosserat rod theory

A fiber jet is a slender long body, i.e. a rod in the context of three-dimensional continuum mechanics. Because of its slender geometry, its dynamics might be reduced to an one-dimensional description by averaging the underlying balance laws over its cross-sections. This procedure is based on the assumption that the displacement field in each cross-section can be expressed in terms of a finite number of vector- and tensor-valued quantities. The most relevant case is the special Cosserat rod theory that consists of only two constitutive elements, a curve specifying the position and an orthonormal director triad characterizing the orientation of the cross-sections. In the following we present the special Cosserat rod theory for a viscous fiber jet in a Lagrangian as well as Eulerian framework.

2.1. Lagrangian framework.

A special Cosserat rod in the three-dimensional Euclidean space $\mathbb{E}^3$ is defined by a curve $\mathbf{r} : Q \to \mathbb{E}^3$ and an orthonormal director triad $\{\mathbf{d_1}, \mathbf{d_2}, \mathbf{d_3}\} : Q \to \mathbb{E}^3$ with $Q = \{(\sigma, t) \in \mathbb{R}^2 \,|\, \sigma \in [\sigma_a(t), \sigma_b(t)],\, t > 0\}$, where σ addresses a material cross-section (material point) of the rod. The domain of the material parameter is chosen to be time-dependent to allow for inflow and outflow boundaries in the Lagrangian description.

The derivatives of the curve $\mathbf{r}$ with respect to time and material parameter are the velocity and the tangent field,

$$\mathbf{v} = \partial_t \mathbf{r}, \qquad \boldsymbol{\tau} = \partial_\sigma \mathbf{r}.$$

Due to the orthonormality of the directors there exist vector-valued functions $\boldsymbol{\omega}$ (angular velocity) and $\boldsymbol{\kappa}$ (generalized curvature) satisfying

$$\partial_t \mathbf{d_k} = \boldsymbol{\omega} \times \mathbf{d_k}, \qquad \partial_\sigma \mathbf{d_k} = \boldsymbol{\kappa} \times \mathbf{d_k}$$

for $k = 1, 2, 3$. The definitions of $\mathbf{v}, \boldsymbol{\tau}$ as well as $\boldsymbol{\omega}, \boldsymbol{\kappa}$ imply the compatibility conditions,

$$\partial_t \boldsymbol{\tau} = \partial_\sigma \mathbf{v}, \qquad \partial_t \boldsymbol{\kappa} = \partial_\sigma \boldsymbol{\omega} + \boldsymbol{\omega} \times \boldsymbol{\kappa}.$$

Combining the kinematic equations with the dynamic ones, i.e. the balance laws for linear and angular momentum, yields the full framework of the special Cosserat rod theory [1]

$$\begin{aligned}\partial_t \mathbf{r} &= \mathbf{v}\\ \partial_t \mathbf{d_k} &= \boldsymbol{\omega} \times \mathbf{d_k}\\ \partial_t \boldsymbol{\tau} &= \partial_\sigma \mathbf{v}\\ \partial_t \boldsymbol{\kappa} &= \partial_\sigma \boldsymbol{\omega} + \boldsymbol{\omega} \times \boldsymbol{\kappa}\\ (\varrho A)\partial_t(\mathbf{v} + \partial_t \mathbf{c}) &= \partial_\sigma \mathbf{n} + \mathbf{f}\\ \partial_t \mathbf{h} + (\varrho A)\mathbf{c} \times \partial_t \mathbf{v} &= \partial_\sigma \mathbf{m} + \boldsymbol{\tau} \times \mathbf{n} + \mathbf{l}\end{aligned} \tag{2.1}$$

equipped with appropriate boundary and initial conditions. The line density (ϱA) is defined as Lagrangian quantity in the reference configuration and is hence time-independent. To complete the system (2.1), the angular momentum line density $\mathbf{h}$ has to be specified in terms of the kinematic quantities by a geometrical model, the contact force and couple $\mathbf{n}$, $\mathbf{m}$ by material laws and the external loads (body force and body couple line density) $\mathbf{f}$, $\mathbf{l}$ by the considered application. The offset field $\mathbf{c}$ is defined such that $\mathbf{r}(\sigma, t) + \mathbf{c}(\sigma, t)$ equals the center of mass in the corresponding material cross-section. We choose $\mathbf{r}$ as the mass-associated center-line, i.e.

$$\mathbf{c} = \mathbf{0}. \tag{2.2}$$

Remark 1. *The first two evolution equations for curve* $\mathbf{r}$ *and triad* $\mathbf{d_k}$ *in* (2.1) *can alternatively be replaced by*

$$\partial_\sigma \mathbf{r} = \boldsymbol{\tau}, \qquad \partial_\sigma \mathbf{d_k} = \boldsymbol{\kappa} \times \mathbf{d_k}, \tag{2.3}$$

which is particularly necessary for stationary considerations, see section 3. Certainly, (2.3) *can also make up for the compatibility conditions for* $\boldsymbol{\tau}$ *and* $\boldsymbol{\kappa}$ *in* (2.1)*.*

Calculus 2. *For the discussion of closure relations and later on for the reformulation of the complete rod model* (2.7)*, we decompose any vector field* $\mathbf{x}$ *of our rod theory in the director basis* $\{\mathbf{d_1}, \mathbf{d_2}, \mathbf{d_3}\}$*. Moreover, we introduce a fixed outer orthonormal basis* $\{\mathbf{e_1}, \mathbf{e_2}, \mathbf{e_3}\}$*, consequently* $\mathbf{x} = \sum_{k=1}^3 x_k \mathbf{d_k} = \sum_{k=1}^3 \bar{x}_k \mathbf{e_k}$*. Note that the corresponding component triples* $\mathsf{x} = (x_1, x_2, x_3)$ *and* $\bar{\mathsf{x}} = (\bar{x}_1, \bar{x}_2, \bar{x}_3) \in \mathbb{R}^3$ *in the director basis and the fixed outer basis respectively are strictly to distinguish from the original field* $\mathbf{x} \in \mathbb{E}^3$ *in the Euclidean vector space.*

The director basis can be transformed into the fixed outer basis by the tensor-valued rotation $\mathbf{D}$*, i.e.* $\mathbf{D} = \mathbf{e_i} \otimes \mathbf{d_i} = D_{ij} \mathbf{e_i} \otimes \mathbf{e_j} \in \mathbb{E}^3 \otimes \mathbb{E}^3$ *with associated orthogonal matrix* $\mathsf{D} = (D_{ij}) = (\mathbf{d_i} \cdot \mathbf{e_j}) \in SO(3)$*. For the coordinate tupels,* $\mathsf{x} = \mathsf{D} \cdot \bar{\mathsf{x}}$ *holds.*

The component triples of the partial derivatives with respect to t *and* σ *in the director basis are*

$$(\partial_t \mathbf{x} \cdot \mathbf{d_k})_{k=1,2,3} = \partial_t \mathsf{x} + \omega \times \mathsf{x}, \qquad (\partial_\sigma \mathbf{x} \cdot \mathbf{d_k})_{k=1,2,3} = \partial_\sigma \mathsf{x} + \kappa \times \mathsf{x}.$$

These relations yield

$$\partial_t \mathsf{D} = -\omega \times \mathsf{D}, \qquad \partial_\sigma \mathsf{D} = -\kappa \times \mathsf{D}.$$

for the derivatives of the rotation matrix. Here, the cross-product $\mathsf{a} \times \mathsf{A} \in \mathbb{R}^{3\times3}$ *between a vector* $\mathsf{a} \in \mathbb{R}^3$ *and a matrix* $\mathsf{A} \in \mathbb{R}^{3\times3}$ *is defined by* $(\mathsf{a} \times \mathsf{A}) \cdot \mathsf{x} = \mathsf{a} \times (\mathsf{A} \cdot \mathsf{x})$ *for all* $\mathsf{x} \in \mathbb{R}^3$*.*

For the geometrical model for $\mathbf{h}$, we need an ansatz how the three-dimensional geometry changes with respect to the deformations of the Cosserat rod. The incompressibility of a three-dimensional viscous jet leads to a shrinking of the cross-sections when stretching the body. During this deformation their shapes are assumed to be retained. Moreover, we restrict to fiber jets with circular cross-sections and constant mass density ϱ in the following. Introducing the dilatation measure $e = \tau_3 = \boldsymbol{\tau} \cdot \mathbf{d_3}$ and the referential cross-sectional area $A_\circ(\sigma)$, our geometrical model yields a angular momentum $\mathbf{h}$ linearly in the angular speed $\boldsymbol{\omega}$ of the specific form

$$\mathbf{h} = \frac{1}{e} \varrho \, \mathbf{J}_\circ \cdot \boldsymbol{\omega}, \quad \mathbf{J}_\circ = J_{ij} \, \mathbf{d_i} \otimes \mathbf{d_j}, \quad \mathsf{J}_\circ = (J_{ij}) = I_\circ \mathrm{diag}(1, 1, 2), \quad I_\circ = \frac{A_\circ^2}{4\pi}. \tag{2.4}$$

Moreover, $(\varrho A) = \varrho A_\circ$ holds. The matrix $\mathsf{J}_\circ$ associated to the tensor-valued moment of inertia $\mathbf{J}_\circ$ is exclusively based on the referential cross-sectional area $A_\circ$ via the definition of the polar moment of inertia $I_\circ$ and is hence time-independent.

Remark 3. *The derivation of the geometrical model* (2.4) *follows straightforward the standard averaging techniques described in* [1] *where we take the following ansatz for the position field of the three-dimensional rod in appropriate Cartesian coordinates*

$$\mathbf{p}(x_1, x_2, \sigma, t) = \mathbf{r}(\sigma, t) + \frac{1}{\sqrt{e(\sigma,t)}}(x_1 \mathbf{d_1}(\sigma, t) + x_2 \mathbf{d_2}(\sigma, t)), \qquad (2.5)$$
$$(x_1,x_2) \in \mathcal{A}_\circ(\sigma) = \{(x_1, x_2) \in \mathbb{R}^2 \,|\, x_1^2 + x_2^2 \leq R_\circ^2(\sigma)\}, \quad A_\circ = \pi R_\circ^2.$$

Allowing time-dependent shrinking, our ansatz (2.5) *differs from the classical one,* $\mathbf{p}(x_1, x_2, \sigma, t) = \mathbf{r}(\sigma, t) + x_1 \mathbf{d_1}(\sigma, t) + x_2 \mathbf{d_2}(\sigma, t)$*, which is standard in the theory of elastic rods* [1]*. It implies that at the same time* $\mathbf{r}$ *is a material curve, i.e.* $\mathbf{p}(0, 0, \sigma, t) = \mathbf{r}(\sigma, t)$ *for all* t*, the mass-associated centerline, i.e.* $\mathbf{c} = \int_{\mathcal{A}_\circ} \mathbf{p}\; \mathrm{d}x_1\; \mathrm{d}x_2/A_\circ - \mathbf{r} = \mathbf{0}$*, and the geometrical center-line, i.e.* $\mathbf{r}(\sigma, t)$ *is the midpoint of the circle* $\mathbf{p}(R_\circ(\sigma) \cos \phi, R_\circ(\sigma) \sin \phi, \sigma, t)$*,* $\phi \in [0, 2\pi[$ *with radius* $R(\sigma, t) = R_\circ(\sigma)/\sqrt{e(\sigma, t)}$*. Moreover, the scaling with the dilatation measure* e *ensures the incompressibility at the center-line, i.e.* $\det \partial_{\mathbf{x}} \mathbf{p}(0, 0, \sigma, t) = 1$*.*

Formulating material laws for the contact force $\mathbf{n}$ and couple $\mathbf{m}$, the objectivity, i.e. the invariance of the laws with respect to spatial translation and rotation as well as to time shifts, plays a very important role. Therefore, it is most elegant to prescribe the constitutive laws in the director basis. The constitutive laws are often combined with algebraic constraints restricting the dynamics. An example is the so-called Kirchhoff constraint $\boldsymbol{\tau} = \mathbf{d_3}$ suppressing shear and forcing inextensibility, then the contact force $\mathbf{n}$ becomes a variable of the system (2.1) – as Lagrangian multiplier to the constraint. For the stretching of viscous fibers, it is necessary to weaken the non-extensibility by introducing a modified Kirchhoff constraint $\boldsymbol{\tau} = e\mathbf{d_3}$, $e > 0$. Then, only the normal contact force components n_1 and n_2 are Lagrangian multipliers, whereas the tangential one n_3 together with the contact couple $\mathbf{m}$ have to be specified by a material law. We use laws that are linear in the rates of the strain variables τ and κ, i.e.

$$\tau = e\mathsf{e}_3 = (0, 0, e), \qquad n_3 = 3\mu A_\circ \frac{\partial_t e}{e^2}, \qquad \mathsf{m} = 3\mu I_\circ \operatorname{diag}(1, 1, 2/3) \cdot \frac{\partial_t \kappa}{e^3}, \quad I_\circ = \frac{A_\circ^2}{4\pi}$$

with dynamic viscosity μ of the fiber (cf. calculus 2). These constitutive laws correspond to the ones Ribe derived in an Eulerian framework, see [16, 17].

In the rotational fiber spinning the external loads rise from gravity, i.e. $\mathbf{f} = \varrho A_\circ g\, \mathbf{e_g}$ and $\mathbf{l} = \mathbf{c} \times \mathbf{f} = \mathbf{0}$.

Remark 4. *Asymptotic analysis of the three-dimensional free boundary fiber spinning problem allows the systematic, formally strict derivation of an one-dimensional viscous model, (see* [6, 5] *for straight and* [13, 12] *for curved fibers in an Eulerian framework). However, the leading-order terms with respect to the slenderness parameter do not result in a Cosserat rod model, but in a string model where all angular momentum effects cancel out. It has the form*

$$\partial_t \mathbf{r} = \mathbf{v}, \qquad \partial_t \boldsymbol{\tau} = \partial_\sigma \mathbf{v}, \qquad \varrho A_\circ\, \partial_t \mathbf{v} = \partial_\sigma \left(n \frac{\boldsymbol{\tau}}{\|\boldsymbol{\tau}\|} \right) + \mathbf{f}, \qquad (2.6)$$

with the same constitutive law for the scalar-valued traction as in the above rod theory, cf. $n = n_3$*,* $\|\boldsymbol{\tau}\| = e$*.*

Summing up, we present the complete rod system for the unknowns $(\bar{\mathsf{r}}, \mathsf{D}, e, \kappa, \mathsf{v}, \omega, n_1, n_2)$ in the director basis

$$\begin{aligned} \mathsf{D} \cdot \partial_t \bar{\mathsf{r}} &= \mathsf{v} \\ \partial_t \mathsf{D} &= -\omega \times \mathsf{D} \\ \partial_t e \mathsf{e}_3 &= \partial_\sigma \mathsf{v} + \kappa \times \mathsf{v} + e \mathsf{e}_3 \times \omega \\ \partial_t \kappa &= \partial_\sigma \omega + \kappa \times \omega \\ \varrho A_\circ \partial_t \mathsf{v} &= \partial_\sigma \mathsf{n} + \kappa \times \mathsf{n} + \varrho A_\circ \mathsf{v} \times \omega + \mathsf{D} \cdot \bar{\mathsf{f}} \\ \rho \mathsf{J}_\circ \cdot \partial_t \frac{\omega}{e} &= \partial_\sigma \mathsf{m} + \kappa \times \mathsf{m} + e \mathsf{e}_3 \times \mathsf{n} + \varrho (\mathsf{J}_\circ \cdot \frac{\omega}{e}) \times \omega \end{aligned} \tag{2.7}$$

with

$$\mathsf{J}_\circ = I_\circ \mathrm{diag}(1,1,2), \qquad n_3 = 3\mu A_\circ \frac{\partial_t e}{e^2}, \qquad \mathsf{m} = 3\mu I_\circ \mathrm{diag}(1,1,2/3) \cdot \frac{\partial_t \kappa}{e^3}, \qquad I_\circ = \frac{A_\circ^2}{4\pi}.$$

Note that the cross-section at a material position σ at time t is given by

$$A(\sigma,t) = \frac{1}{e(\sigma,t)} A_\circ(\sigma)$$

in consequence of the geometrical model. The reference area $A_\circ$ might be replaced by the actual area A in (2.7), which implies the inclusion of an additional evolution equation

$$\partial_t (eA) = 0$$

with appropriate initial condition. In this context, we further introduce $I(\sigma,t) = I_\circ(\sigma)/e^2(\sigma,t)$ as the actual polar moment of inertia and $\mathsf{J} = I\mathrm{diag}(1,1,2)$ as the corresponding matrix.

2.2. **Eulerian framework.** System (2.7) is formulated in a Lagrangian setting. Thereby, the material parameterization might be determined up to orientation and a constant by an arc-length parameterized reference configuration. Alternatively, any other time-dependent parameterization could be used for the formulation of the Cosserat theory, defined via an orientated bijective mapping

$$S(\cdot,t) : [\sigma_a(t), \sigma_b(t)] \to [S(\sigma_a(t),t), S(\sigma_b(t),t)] = [s_a(t), s_b(t)], \quad \sigma \mapsto S(\sigma,t).$$

Assuming sufficient regularity, a scalar convective velocity $\tilde{u}$ and spatial Jacobian j belongs to S,

$$\partial_t S(\sigma,t) = \tilde{u}(S(\sigma,t),t), \qquad \partial_\sigma S(\sigma,t) = j(\sigma,t) > 0,$$

for which the following compatibility condition holds

$$\partial_s \tilde{u}(S(\sigma,t),t) = \frac{\partial_t j}{j}(\sigma,t).$$

Calculus 5. *For the definition of the rod-associated fields and the conservation of their physical meaning in an other parameterization, we introduce the formalism of so-called type-n-fields, $n \in \mathbb{Z}$, that are transformed according to*

$$j^n(\sigma,t) \tilde{f}(S(\sigma,t),t) = f(\sigma,t)$$

where $f(\sigma,t)$ and $\tilde{f}(s,t)$ denote a type-n-field in the material and the new parameters, respectively. In the following we treat $\bar{\mathsf{r}}$, D, A, v, ω, n, $\mathsf{m}, \mathsf{J}, I$ as type-0-fields and e, κ, f as type-1-fields. The transformation of (2.7) requires the computation of certain derivatives with respect to t and σ. In particular, we need

$$\begin{aligned} &\partial_t f(\sigma,t) = (\partial_t \tilde{f} + \tilde{u}\partial_s \tilde{f})(S(\sigma,t),t) \quad \textit{and} \quad \partial_\sigma f(\sigma,t) = j(\sigma,t)\, \partial_s \tilde{f}(S(\sigma,t),t) && \textit{for type-0-fields} \\ &\partial_t f(\sigma,t) = j(\sigma,t)\, (\partial_t \tilde{f} + \partial_s(\tilde{u}\tilde{f}))(S(\sigma,t),t) && \textit{for type-1-fields.} \end{aligned}$$

Considering j as type-1-field yields consistently $\tilde{j} = 1$ by definition.

The re-parameterization of all fields carries convective terms with speed $\tilde{u}$ into (2.7). Choosing $\tilde{u} = 0$ implies a material description. Instead of imposing $\tilde{u}$ explicitly, a constraint might alternatively be prescribed so that $\tilde{u}$ becomes the associated Lagrangian multiplier and hence an additional unknown of the system. A well-known constraint is the arc-length parameterization of the fiber curve for all times, $\tilde{e} = \|\tilde{\boldsymbol{\tau}}\| = \tilde{j} = 1$, that yields an Eulerian setting. Here, $e = j = \partial_\sigma S$ coincides. Moreover, $\partial_t S(\sigma, t) = \tilde{u}(S(\sigma, t), t)$ prescribes the rate of change of the arc-length $S(\sigma, t)$ to the material point σ, e is a measure for the strain and $\partial_s \tilde{u}(S(\sigma, t), t) = (\partial_t e/e)(\sigma, t)$ the corresponding relative strain rate. The Eulerian (spatial) description is undoubtedly the most intuitive one for flow problems and allows the transition to stationary flow considerations. Suppressing the notation $\tilde{}$ for readability in the following, the Cosserat rod theory in Eulerian parameterization is given by

$$\begin{aligned}
\mathsf{D} \cdot \partial_t \bar{\mathsf{r}} &= \mathsf{v} - u\mathsf{e}_3 \\
\partial_t \mathsf{D} &= -(\omega - u\kappa) \times \mathsf{D} \\
\partial_s (u\mathsf{e}_3) &= \partial_s \mathsf{v} + \kappa \times \mathsf{v} + \mathsf{e}_3 \times \omega \\
\partial_t \kappa + \partial_s (u\kappa) &= \partial_s \omega + \kappa \times \omega \\
\partial_t A + \partial_s (uA) &= 0 \\
\rho\partial_t (A\mathsf{v}) + \rho\partial_s (uA\mathsf{v}) &= \partial_s \mathsf{n} + \kappa \times \mathsf{n} + \rho A\mathsf{v} \times \omega + \mathsf{D} \cdot \bar{\mathsf{f}} \\
\rho\partial_t (\mathsf{J} \cdot \omega) + \rho\partial_s (u\mathsf{J} \cdot \omega) &= \partial_s \mathsf{m} + \kappa \times \mathsf{m} + \mathsf{e}_3 \times \mathsf{n} + (\rho\mathsf{J} \cdot \omega) \times \omega
\end{aligned} \tag{2.8}$$

with

$$\mathsf{J} = I\mathrm{diag}(1,1,2), \qquad n_3 = 3\mu A \partial_s u, \qquad \mathsf{m} = 3\mu I \mathrm{diag}(1,1,2/3) \cdot (\partial_s \omega + \kappa \times \omega), \qquad I = \frac{A^2}{4\pi}.$$

Remark 6. *Our system* (2.8) *differs from the rod model that Ribe* [16, 17] *originally proposed and investigated for viscous rope coiling in a lacking term in the angular momentum balance. In our terminology, Ribe's equation has an additional term* $a = A/(4\pi)(\kappa \times \mathsf{e}_3) \times (\partial_s \mathsf{n} + \kappa \times \mathsf{n} + \mathsf{D} \cdot \bar{\mathsf{f}})$ *on the right-hand side which can be traced back to the choice of a non-zero offset function in Lagrange description,*

$$\mathbf{c} = -\frac{A_\circ}{4\pi} \frac{\boldsymbol{\kappa} \times \mathbf{d_3}}{e^2}, \tag{2.9}$$

cf. (2.1). *However, no corresponding term occurs in his linear momentum equation.*

In the embedding into the three-dimensional theory (cf. remark 3), the offset function (2.9) *might be interpreted as consequence of an improved incompressibility model. The underlying ansatz for the position field of the three-dimensional rod in Cartesian coordinates*

$$\mathbf{p}(x_1, x_2, \sigma, t) = \mathbf{r}(\sigma, t) + \frac{1}{\sqrt{e(\sigma, t)}}(x_1 \mathbf{d_1}(\sigma, t) + x_2 \mathbf{d_2}(\sigma, t)) + \frac{x_1^2 + x_2^2 - A_\circ(\sigma)/\pi}{2e^2(\sigma, t)} \boldsymbol{\kappa} \times \mathbf{d_3},$$
$$(x_1, x_2) \in \mathcal{A}_\circ(\sigma) = \{(x_1, x_2) \in \mathbb{R}^2 \,|\, x_1^2 + x_2^2 \leq R_\circ^2(\sigma)\}, \quad A_\circ = \pi R_\circ^2.$$

ensures not only the incompressibility at $\mathbf{r}$ *as our ansatz* (2.5), *but also as linear approximation in its surrounding, i.e.* $\det \partial_\mathbf{x} \mathbf{p}(\epsilon x_1, \epsilon x_2, \sigma, t) = 1 + \mathcal{O}(\epsilon^2)$. *Additionally, it still treats the rod curve* $\mathbf{r}$ *as geometrical center-line in agreement to Ribe's assumption. Hence, the improved incompressibility model implies linear and angular momentum equations that both contain offset-associated terms,* (2.1), (2.9). *In this context Ribe's model can be viewed as simplification for* $A_\circ \ll 1$, *where all terms of* $\mathcal{O}(A_\circ^2)$ *in the linear momentum balance and of* $\mathcal{O}(A_\circ^3)$ *in the angular momentum balance are neglected. However, note that this deduction lacks asymptotic consistency, since the coupling of both equations generates additional terms of* $\mathcal{O}(A_\circ^2)$ *in the linear momentum equation. Consequently, the consideration of all terms of* $\mathcal{O}(A_\circ^2)$ *seems to be necessary to obtain an one order higher incompressible rod model than* (2.8).

For the numerical comparison of (2.8) *and Ribe's model we refer to section 4.*

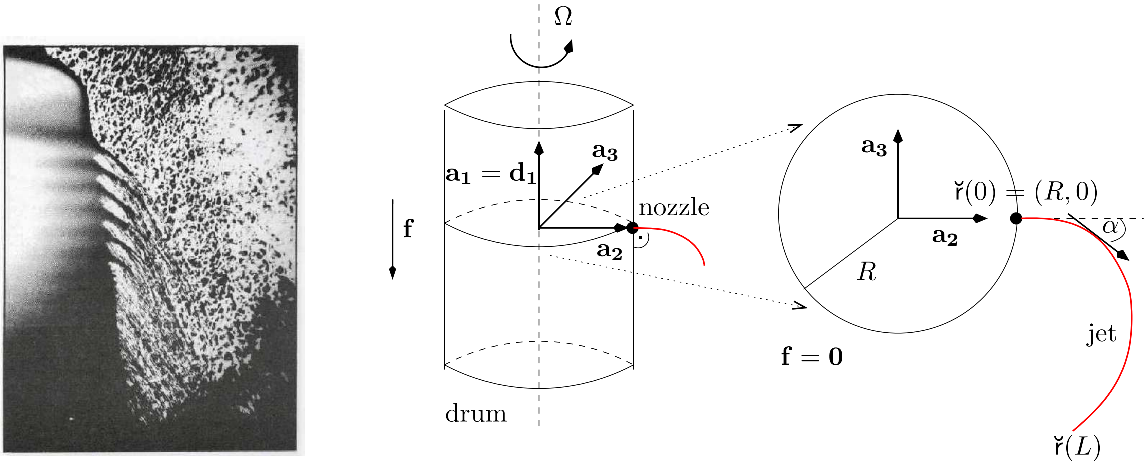

FIGURE 3.1. *Left*: Rotational fiber spinning process, photo by industrial partner. *Right*: Sketch of three-dimensional set-up and its two-dimensional simplification under the neglect of gravity.

3. MODELS FOR ROTATIONAL SPINNING

In this section we apply the special Cosserat theory to rotational spinning processes. In these processes, a viscous liquid jet leaves a small spinning nozzle located on the curved face of a circular cylindrical drum rotating about its symmetry axis, cf. figure 3.1. At the nozzle, the velocity, cross-sectional area, direction and curvature of the jet are prescribed. Starting from an initial length of zero, the extruded liquid jet grows and moves due to viscous friction, surface tension and gravity. To describe the process, we choose a coordinate system rotating with the drum. This makes the position of the nozzle and the direction of the inflow time-independent, but introduces fictitious rotational body forces due to inertia. Since the curling behavior of the jet at the nozzle in dependence of fiber viscosity and rotational frequency of the drum is of special interest, we will focus on a simplified, stationary two-dimensional situation, neglecting surface tension, gravity and considering a spun fiber of certain length with stress-free end in the following.

Let $\mathbf{\Omega}$ be the angular frequency of the rotating device, then we introduce the rotating outer basis $\{\mathbf{a_1}(t), \mathbf{a_2}(t), \mathbf{a_3}(t)\}$ satisfying $\partial_t \mathbf{a_i} = \mathbf{\Omega} \times \mathbf{a_i}$, $i = 1, 2, 3$. We indicate the corresponding coordinate tupel to an arbitrary vector field $\mathbf{x} = \sum_{i=1}^{3} \breve{x}_i \mathbf{a_i} \in \mathbb{E}^3$ by $\breve{\mathsf{x}} = (\breve{x}_1, \breve{x}_2, \breve{x}_3) \in \mathbb{R}^3$. Analogously to calculus 2, the director basis can be transformed into the rotating outer basis by the tensor-valued rotation $\mathbf{R}$, i.e. $\mathbf{R} = \mathbf{a_i} \otimes \mathbf{d_i} = R_{ij} \mathbf{a_i} \otimes \mathbf{a_j} \in \mathbb{E}^3 \otimes \mathbb{E}^3$ with associated orthogonal matrix $\mathsf{R} = (R_{ij}) = (\mathbf{d_i} \cdot \mathbf{a_j}) \in SO(3)$. For the coordinate tupels, $\mathsf{x} = \mathsf{D} \cdot \bar{\mathsf{x}} = \mathsf{R} \cdot \breve{\mathsf{x}}$ holds. Furthermore, we introduce an adapted velocity and angular speed by

$$\mathbf{v}_\Omega = \mathbf{v} - (\mathbf{\Omega} \times \mathbf{r}), \qquad \boldsymbol{\omega}_\Omega = \boldsymbol{\omega} - \mathbf{\Omega}.$$

Then, skipping the subscript $_\Omega$, our rod model (2.8) gets the form

$$\begin{aligned}
\mathsf{R} \cdot \partial_t \breve{\mathsf{r}} &= \mathsf{v} - u \mathsf{e}_3 \\
\partial_t \mathsf{R} &= -(\omega - u\kappa) \times \mathsf{R} \\
\partial_s (u \mathsf{e}_3) &= \partial_s \mathsf{v} + \kappa \times \mathsf{v} + \mathsf{e}_3 \times \omega \\
\partial_t \kappa + \partial_s (u\kappa) &= \partial_s \omega + \kappa \times \omega \\
\partial_t A + \partial_s (uA) &= 0 \\
\rho \partial_t (A\mathsf{v}) + \rho \partial_s (uA\mathsf{v}) &= \partial_s \mathsf{n} + \kappa \times \mathsf{n} + \rho A \mathsf{v} \times \omega - 2\rho A (\mathsf{R} \cdot \breve{\Omega}) \times \mathsf{v} - \rho A \mathsf{R} \cdot (\breve{\Omega} \times (\breve{\Omega} \times \breve{\mathsf{r}})) + \mathsf{R} \cdot \breve{\mathsf{f}} \\
\rho \partial_t (\mathsf{J} \cdot \omega) + \rho \partial_s (u \mathsf{J} \cdot \omega) &= \partial_s \mathsf{m} + \kappa \times \mathsf{m} + \mathsf{e}_3 \times \mathsf{n} + (\rho \mathsf{J} \cdot (\omega + \mathsf{R} \cdot \breve{\Omega})) \times (\omega + \mathsf{R} \cdot \breve{\Omega}) \\
&\quad + \rho \mathsf{J} \cdot (\omega \times \mathsf{R} \cdot \breve{\Omega}) + \rho \mathsf{J} \cdot \mathsf{R} \cdot \breve{\Omega}\, \partial_s u
\end{aligned} \tag{3.1}$$

with

$$\mathsf{J} = I\mathrm{diag}(1,1,2), \qquad n_3 = 3\mu A\partial_s u, \qquad \mathsf{m} = 3\mu I\mathrm{diag}(1,1,2/3)\cdot(\partial_s\omega + \kappa\times\omega), \qquad I = \frac{A^2}{4\pi}.$$

Neglecting gravity $\mathbf{f} = \mathbf{0}$, the fiber jet stays and moves exclusively in the exit plane perpendicular to the rotation axis of the device for appropriate initial and boundary conditions, figure 3.1. We particularly set $\boldsymbol{\Omega}\|\mathbf{d_1}$ and $\mathbf{d_1} = \mathbf{a_1}$ so that the rotation is prescribed by a single angle $\alpha \in [0, 2\pi[$. Then, the quantities $\mathbf{r}$, $\mathbf{v}$, $\mathbf{n}$ play in the $\mathbf{d_2}$-$\mathbf{d_3}$-plane, whereas $\boldsymbol{\kappa}$, $\boldsymbol{\omega}$ and $\mathbf{m}$ are parallel to $\mathbf{d_1}$ as consequence of the kinematic equations and the material law. The coordinate terminology simplifies in this two-dimensional set-up, we use e.g. $\mathsf{v} = (v_2, v_3)$, $\mathsf{v}^\perp = (-v_3, v_2)$ and $\omega = \omega_1$, analogously for the other quantities above. With $\Omega = \Omega_1$ and rotation matrix

$$\mathsf{R}(\alpha) = \begin{pmatrix} \sin\alpha & -\cos\alpha \\ \cos\alpha & \sin\alpha \end{pmatrix},$$

the two-dimensional Cosserat model reads after renumbering (i.e. (x_2, x_3) turns into (x_1, x_2) for all coordinate tupels x)

$$\begin{aligned}
\mathsf{R}(\alpha)\cdot\partial_t\check{\mathsf{r}} &= \mathsf{v} - u\mathsf{e}_2 \\
\partial_t\alpha &= \omega - u\kappa \\
\partial_s(u\mathsf{e}_2) &= \partial_s\mathsf{v} + \kappa\mathsf{v}^\perp + \omega\mathsf{e}_1 \\
\partial_t\kappa + \partial_s(u\kappa) &= \partial_s\omega \\
\partial_t A + \partial_s(uA) &= 0 \\
\rho\partial_t(A\mathsf{v}) + \rho\partial_s(uA\mathsf{v}) &= \partial_s\mathsf{n} + \kappa\mathsf{n}^\perp - \rho A\omega\mathsf{v}^\perp - 2\rho A\Omega\mathsf{v}^\perp + \rho A\Omega^2\mathsf{R}(\alpha)\cdot\check{\mathsf{r}} \\
\rho\partial_t(I\omega) + \rho\partial_s(uI\omega) &= \partial_s m - n_1 + \rho I\Omega\,\partial_s u
\end{aligned} \tag{3.2}$$

with

$$n_2 = 3\mu A\partial_s u, \qquad m = 3\mu I\partial_s\omega, \qquad I = \frac{A^2}{4\pi}.$$

In the transition to stationarity, the mass flux becomes constant, i.e. $uA = Q/\rho = const$. Moreover, the first two equations of (3.2) loose their evolution character and yield instead explicit relations for the kinematic quantities, $\mathsf{v} = u\mathsf{e}_2$ and $\omega = u\kappa$, which consistently fulfill the third and fourth equation. Therefore, we follow remark 1 and incorporate alternatively the equations for the spatial derivatives of curve and angle, $\partial_s\check{\mathsf{r}} = \chi(\alpha)$ and $\partial_s\alpha = \kappa$ using $\chi(\alpha) = (\cos\alpha, \sin\alpha)$, $\chi(\alpha)^\perp = (-\sin\alpha, \cos\alpha)$. In terms of a first order system for $\check{\mathsf{r}}, \alpha, \kappa, u, n_1, n_2, m$ supplemented with geometric and kinematic boundary conditions at the nozzle ($s = 0$) and stress-free dynamic boundary conditions at a certain fiber length ($s = L$), we finally obtain the following boundary value problem

$$\begin{aligned}
\partial_s\check{\mathsf{r}} &= \chi(\alpha), & \check{\mathsf{r}}(0) &= (R, 0) \\
\partial_s\alpha &= \kappa, & \alpha(0) &= 0 \\
\partial_s\kappa &= \frac{4\pi\rho^2}{3\mu Q^2}um - \frac{\rho}{3\mu Q}\kappa n_2, & \kappa(0) &= 0 \\
\partial_s u &= \frac{\rho}{3\mu Q}un_2, & u(0) &= u_0 \\
\partial_s n_1 &= \kappa n_2 - Q\kappa u + Q\Omega^2\frac{1}{u}\check{\mathsf{r}}\cdot\chi(\alpha)^\perp - 2Q\Omega, & n_1(L) &= 0 \\
\partial_s n_2 &= \frac{\rho}{3\mu}un_2 - \kappa n_1 - Q\Omega^2\frac{1}{u}\check{\mathsf{r}}\cdot\chi(\alpha), & n_2(L) &= 0 \\
\partial_s m &= \frac{\rho}{3\mu}um + n_1 - \frac{Q}{12\pi\mu}\left(\frac{\Omega}{u} + \kappa\right)n_2 & m(L) &= 0.
\end{aligned} \tag{3.3}$$

System (3.3) contains seven physical parameters, i.e. fiber density ρ, viscosity μ, length L, diameter d_0 and velocity u_0 at the nozzle as well as drum radius R and rotational frequency Ω. These induce four dimensionless numbers characterizing the fiber spinning: Reynolds number $\mathrm{Re} = \rho u_0 R/\mu$ as ratio between inertia and viscosity, Rossby number $\mathrm{Rb} = u_0/(\Omega R)$ as ratio between inertia and rotation as well as $l = L/R$ and $\epsilon = d_0/R$ as length ratios between fiber length, -diameter respectively and drum radius. For the subsequent numerical investigation of viscous and rotational effects on the fiber behavior, we non-dimensionalize (3.3) by help of the following reference values: $s_0 = r_0 = R$, $\alpha_0 = 1$, $\kappa_0 = R^{-1}$, $u_0 = u_0$, $n_0 = \pi\mu d_0^2 u_0/(4R) = \rho u_0^2 R^2 \epsilon^2/(4\mathrm{Re})$, $m_0 = \pi\mu d_0^4 u_0/(16R^2) = \rho u_0^2 R^3 \epsilon^4/(16\mathrm{Re})$. The last two scalings are motivated by the material laws and the fact that $Q/\rho = Au$. This gives

$$
\begin{aligned}
\partial_s \check{\mathbf{r}} &= \chi(\alpha), & \check{\mathbf{r}}(0) &= (1,0)\\
\partial_s \alpha &= \kappa, & \alpha(0) &= 0\\
\partial_s \kappa &= \frac{4}{3}um - \frac{1}{3}\kappa n_2, & \kappa(0) &= 0\\
\partial_s u &= \frac{1}{3}un_2, & u(0) &= 1\\
\partial_s n_1 &= \kappa n_2 - \mathrm{Re}\kappa u + \frac{\mathrm{Re}}{\mathrm{Rb}^2}\frac{1}{u}\check{\mathbf{r}}\cdot\chi(\alpha)^\perp - \frac{2\mathrm{Re}}{\mathrm{Rb}}, & n_1(l) &= 0\\
\partial_s n_2 &= \frac{\mathrm{Re}}{3}un_2 - \kappa n_1 - \frac{\mathrm{Re}}{\mathrm{Rb}^2}\frac{1}{u}\check{\mathbf{r}}\cdot\chi(\alpha), & n_2(l) &= 0\\
\partial_s m &= \frac{\mathrm{Re}}{3}um + \frac{4}{\epsilon^2}n_1 - \frac{\mathrm{Re}}{12\mathrm{Rb}}\frac{n_2}{u} - \frac{\mathrm{Re}}{12}\kappa n_2 & m(l) &= 0.
\end{aligned}
\tag{3.4}
$$

Remark 7. *Comparing with Ribe's rod model, his offset modification (cf. remark 6) leads to two additional terms* $Q/(12\pi\mu)\kappa n_2 - (Q^2\Omega^2)/(4\pi\rho)\kappa/u^2\,\check{\mathbf{r}}\cdot\chi(\alpha)$ *in the angular momentum equation of* (3.3)*, where the first one cancels out an already existing one. Hence, the resulting non-dimensionalized equation*

$$\partial_s m = \frac{\mathrm{Re}}{3}um + \frac{4}{\epsilon^2}n_1 - \frac{\mathrm{Re}}{12\mathrm{Rb}}\frac{n_2}{u} - \frac{\mathrm{Re}}{4\mathrm{Rb}^2}\frac{\kappa}{u^2}\check{\mathbf{r}}\cdot\chi(\alpha)$$

differs from our model (3.4) *only in the last term.*

In the limit $\epsilon \to 0$, the normal force vanishes ($n_1 = 0$) and the angular momentum effects decouple. The rod model (3.4) reduces to a string model for $\check{\mathbf{r}}, \alpha, u, n$ with traction force $n = n_2$,

$$
\begin{aligned}
\partial_s \check{\mathbf{r}} &= \chi(\alpha), & \check{\mathbf{r}}(0) &= (1,0)\\
\left(u - \frac{1}{\mathrm{Re}}n\right)\partial_s \alpha &= \frac{1}{\mathrm{Rb}^2}\frac{1}{u}\check{\mathbf{r}}\cdot\chi(\alpha)^\perp - \frac{2}{\mathrm{Rb}}, & \alpha(0) &= 0\\
\partial_s u &= \frac{1}{3}un, & u(0) &= 1\\
\partial_s n &= \frac{\mathrm{Re}}{3}un - \frac{\mathrm{Re}}{\mathrm{Rb}^2}\frac{1}{u}\check{\mathbf{r}}\cdot\chi(\alpha), & n(l) &= 0.
\end{aligned}
\tag{3.5}
$$

Note that this string model stands in accordance to the result (2.6) in remark 4 that was asymptotically derived from the three-dimensional instationary incompressible Navier-Stokes equations describing the rotational spinning as free boundary value problem for a Newtonian fluid, see [13] and its extension to surface tension [12]. Moreover, first investigations of (3.5) have been performed for the given stationary two-dimensional set-up regarding $\mathrm{Rb} \ll 1$ and $\mathrm{Re}^{-1} \ll 1$, [10].

4. Numerical investigations

According to the studies in [10], the string model (3.5) allows no physically relevant solutions for $\mathrm{Rb}^2 < \mathrm{Re}^{-1}$ with $\mathrm{Rb} \ll 1$ and $\mathrm{Re}^{-1} \ll 1$. However, the spinning of less and highly viscous fibers under fast rotations is daily routine in industry. Therefore, we will investigate the rod model (3.4) numerically in view of performance, validity and applicability in this section. In particular, we will show that the rod model not only covers the string model but also goes far beyond and opens up new parameter ranges of practical interest.

4.1. **Numerical method.** For the numerical handling of the boundary value problems (3.4) and (3.5), systems of non-linear equations are set up via a Runge-Kutta collocation method and solved by a Newton method. The convergence of the Newton method depends thereby crucially on the initial guess. An appropriate guess for the rod model (3.4) turns out to be the solution of the limit case $\epsilon \to 0$ for suitable parameters $(\mathrm{Re}, \mathrm{Rb})$. Hence, the solution of the string model (3.5) is taken as initial guess for $(\check{\mathfrak{r}}, \alpha, u, n = n_2)$ which is supplemented with

$$\begin{aligned} n_1 &= 0 \\ \kappa &= \left(\frac{1}{\mathrm{Rb}^2}\frac{1}{u}\check{\mathfrak{r}} \cdot \chi(\alpha)^\perp - \frac{2}{\mathrm{Rb}}\right) \Big/ \left(u - \frac{n_2}{\mathrm{Re}}\right) \\ m &= \frac{1}{4u}(3\partial_s \kappa + \kappa n_2). \end{aligned}$$

The expressions for κ and m come from the differential equations for n_1 and κ in (3.4), respectively, using $n_1 = 0$. However, solving the string model (3.5) itself also requires an initial guess. This might be taken from the inviscid limit case $\mathrm{Re} \to \infty$, according to [10]. A good approximation is

$$\begin{aligned} \check{\mathfrak{r}}(s) &= \begin{pmatrix} 1 & \sqrt{2s} \\ \sqrt{2s} & -1 \end{pmatrix} \cdot \chi(\sqrt{2s}) \\ \alpha(s) &= -\sqrt{2s} \\ u(s) &= \frac{1}{\mathrm{Rb}}\sqrt{2s + \mathrm{Rb}^2} \\ n(s) &= 0 \end{aligned}$$

which is the inviscid solution for $\check{\mathfrak{r}}, \alpha, n$ for $\mathrm{Rb} \to 0$. The small modification from the inviscid solution $u(s) = \sqrt{2s}/\mathrm{Rb}$ ensures the satisfaction of the boundary condition $u(0) = 1$, while keeping the property $\lim_{\mathrm{Rb}\to 0} \mathrm{Rb}\, u(s) = \sqrt{2s}$.

Remark 8. *To improve the computational performance it makes sense to adapt the initial guess iteratively by solving a sequence of boundary value problems with slightly changed parameters* $(\mathrm{Re}, \mathrm{Rb})$ *starting from the prescribed one above.*

4.2. **Applicability of rod and string model.** The applicability of the string model (3.5) has obviously limits as the work [10] on inviscid fibers shows. We observe similar failure for viscous fibers exposed to fast rotations, $\mathrm{Re} \ll 1$, $\mathrm{Rb} \ll 1$. The reason lies in the term on the left-hand side of the evolution equation for α, i.e.

$$q(s) = u(s) - \frac{1}{\mathrm{Re}} n(s)$$

that can be interpreted as sum of inertia and viscous energy. It is monotonically increasing on $[0, l]$ and $q(l) > 0$ since $u > 0$. Hence, two cases have to be distinguished: $q(0) > 0$ and $q(0) \le 0$. The first case indicates a inertia-dominated regime, $q > 0$, for which the boundary value problem is well-posed and the numerical simulations yield reasonable results. The second case implies $q(s^\star) = 0$ for $s^\star \in [0, l[$. We have a transition from a viscous to an inertial regime, where the numerical solution breaks down. The system with the prescribed boundary conditions is inconsistent. There are ideas to overcome this problem by modifying the boundary conditions, in particular releasing $\alpha(0) = 0$ see [11]. However, the choice of the boundary conditions is physically reasonable.

The handling of both regimes turns out to be no problem for the complexer rod model (3.4). The boundary value problem is well-posed for $\epsilon \neq 0$ and permits the numerical solution. Containing additional degrees of freedom via the angular momentum consideration allows the prescription of exit angle and curvature at the nozzle, $\alpha(0) = 0$ and $\kappa(0) = 0$, and especially the resolution of the curling behavior near the nozzle. Concerning the applicability of the rod model and its superiority to a string model, our experiences for the rotational spinning are in accordance with the observations for the fluid-mechanical sewing machine in [18].

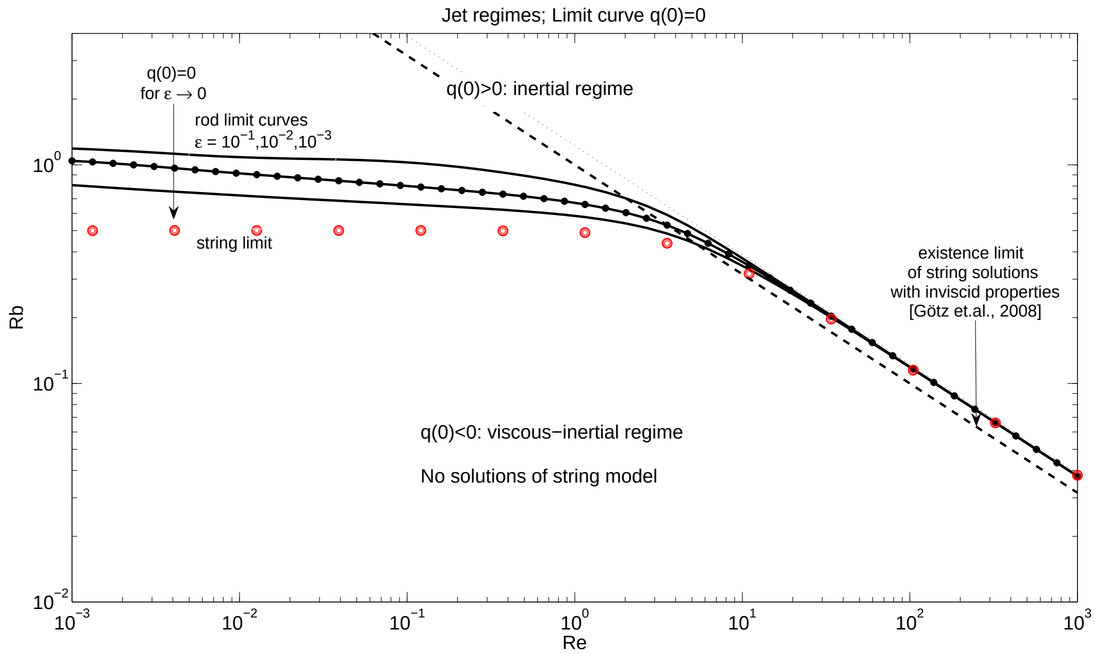

FIGURE 4.2. Jet regimes for varying (Re, Rb)-ranges. Illustration of limit curve $q(0;\mathrm{Re},\mathrm{Rb},\epsilon) = 0$ for the different models: rod model for $\epsilon = 10^{-1}, 10^{-2}, 10^{-3}$ as solid lines (–), Ribe's approach for $\epsilon = 10^{-2}$ with marker ($\star$) and string model with red (o). The string results are of accuracy $tol = 10^{-3}$. The analytical estimate for non-existence of string solutions with inviscid properties, $\mathrm{Rb}^2\mathrm{Re} = 1$, is plotted as dashed line (- -), the actual numerical observation, $\mathrm{Rb}^2\mathrm{Re} = 3/2$, as dotted line (:), [10].

Limit curve. Investigating the two jet regimes in the following, figure 4.2 illustrates the limit curve $q(0;\mathrm{Re},\mathrm{Rb},\epsilon) = 0$ for the rod and string model. Obviously, the curves corresponding to our ϵ-dependent rod model converge to the string limit as $\epsilon \to 0$. Moreover, the limit curves of our and Ribe's rod approach coincide for all $\epsilon > 0$, as exemplified for $\epsilon = 10^{-2}$ in figure 4.2. The slenderness ratio ϵ plays a crucial role for viscous jets of $\mathrm{Re} < 10$, we find $\lim_{\mathrm{Re}\to 0} q(0;\mathrm{Re}, 0.5, 0) = 0$. For non-viscous jets, in contrast, the limit curves are ϵ-independent. They particularly fall together with the non-existence estimate of physically relevant string solutions, $\mathrm{Rb}^2\mathrm{Re} < 1$, for $\mathrm{Re}^{-1} \ll 1$ in [10]. This estimate was derived under the assumptions that the fiber jet is accelerated out off the nozzle and bends in the sense of the drum rotation, $\partial_s u(0) \geq 0$ and $\partial_s \alpha(0) < 0$ yielding $q(0) \in]0, 1]$, in combination with the convexity of the Lagrangian velocity at the nozzle. The last is true in the inviscid case $\mathrm{Re} \to \infty$, where the acceleration of the Lagrangian fluid particle increases with its flight time. Its application to non-viscous jets of $\mathrm{Re}^{-1} \ll 1$ might explain the slight difference of the theoretical estimate in comparison to the numerical results $\mathrm{Rb}^2\mathrm{Re} < 3/2$, as already observed in [10].

To determine the limit curve (root of q) we use a combination of bisection, secant and inverse quadratic interpolation approaches. The nonlinear boundary value problem in the inner loop is solved via the Newton method on top of the Runge-Kutta collocation method according to section 4.1. Thereby, we compute the initial guess iteratively to ensure the convergence of the Newton method. In the case of the string model, we particularly test against the non-solvability of the problem, yielding an accuracy of the string results of order $\mathcal{O}(10^{-3})$.

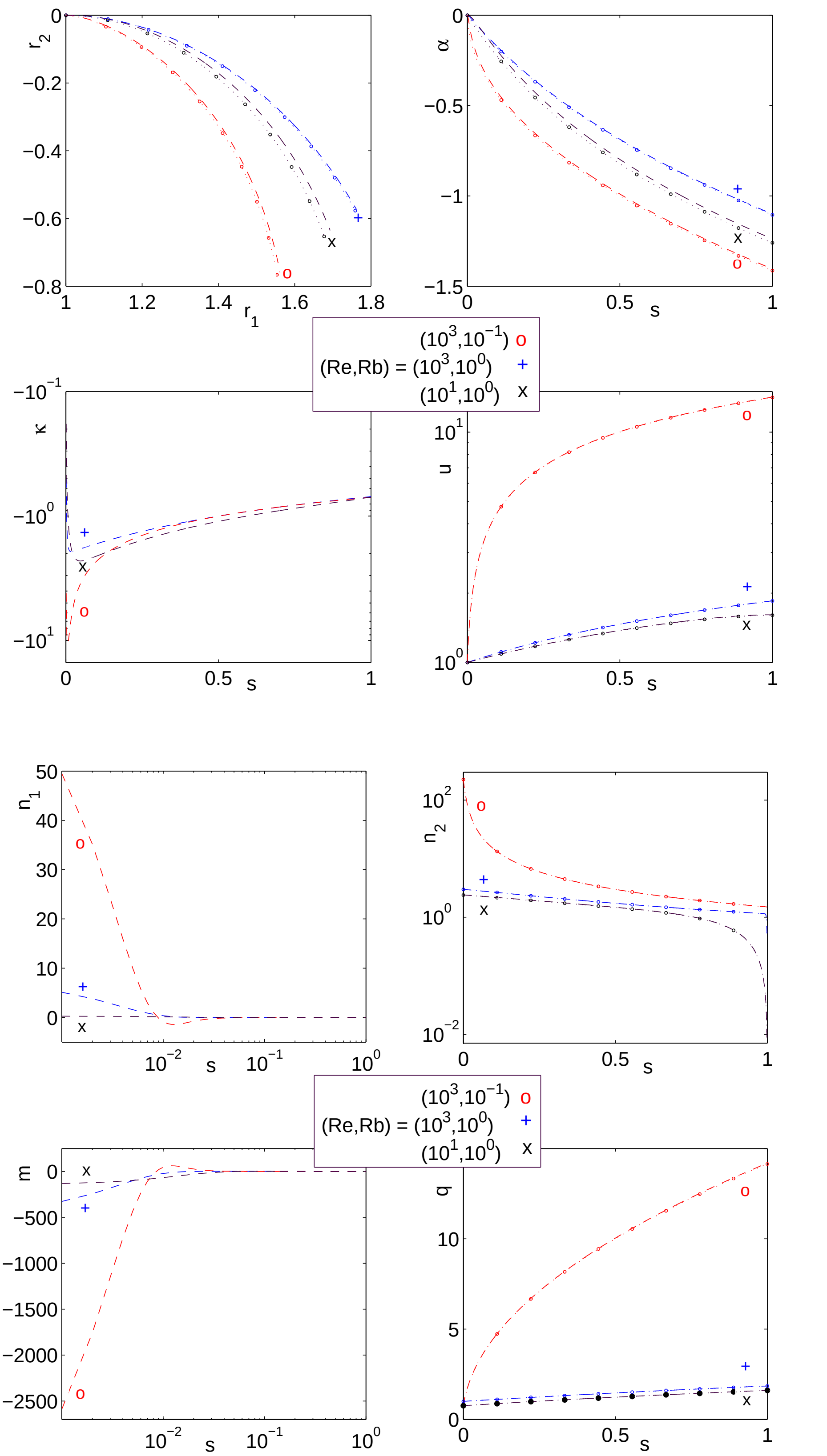

FIGURE 4.3. High Reynolds number inertial jet regime. Rod solution for $\epsilon = 10^{-2}$ is plotted as dashed line (--) and respective string quantities, $\check{\mathrm{r}}, \alpha, u, n = n_2, q$, as dotted line ($\bullet$:) for the cases $(\mathrm{Re}, \mathrm{Rb}) \in \{(1000, 0.1), (1000, 1), (10, 1)\}$ specified with {o,+,x}.

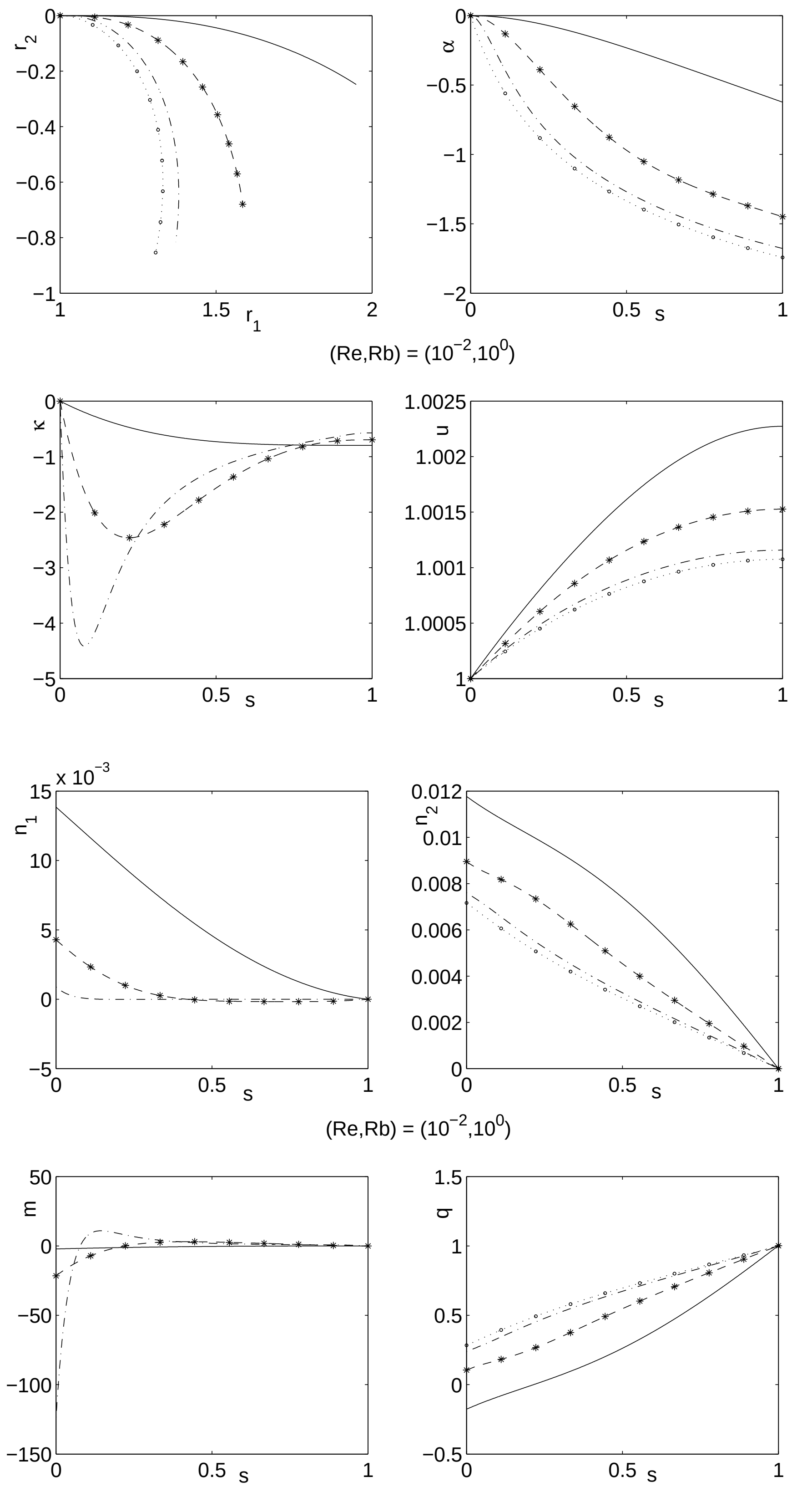

FIGURE 4.4. Low Reynolds number inertial jet regime. Rod solutions for $\epsilon = 10^{-1}, 10^{-2}, 10^{-3}$ are plotted as solid (–), dashed (- -), dash-dotted (-:) lines, respectively, and string quantities, $\check{\mathrm{r}}, \alpha, u, n = n_2, q$, as dotted line (•:) for $(\mathrm{Re}, \mathrm{Rb}) = (0.01, 1)$. Ribe's rod solution for $\epsilon = 10^{-2}$ is marked with ($\star$).

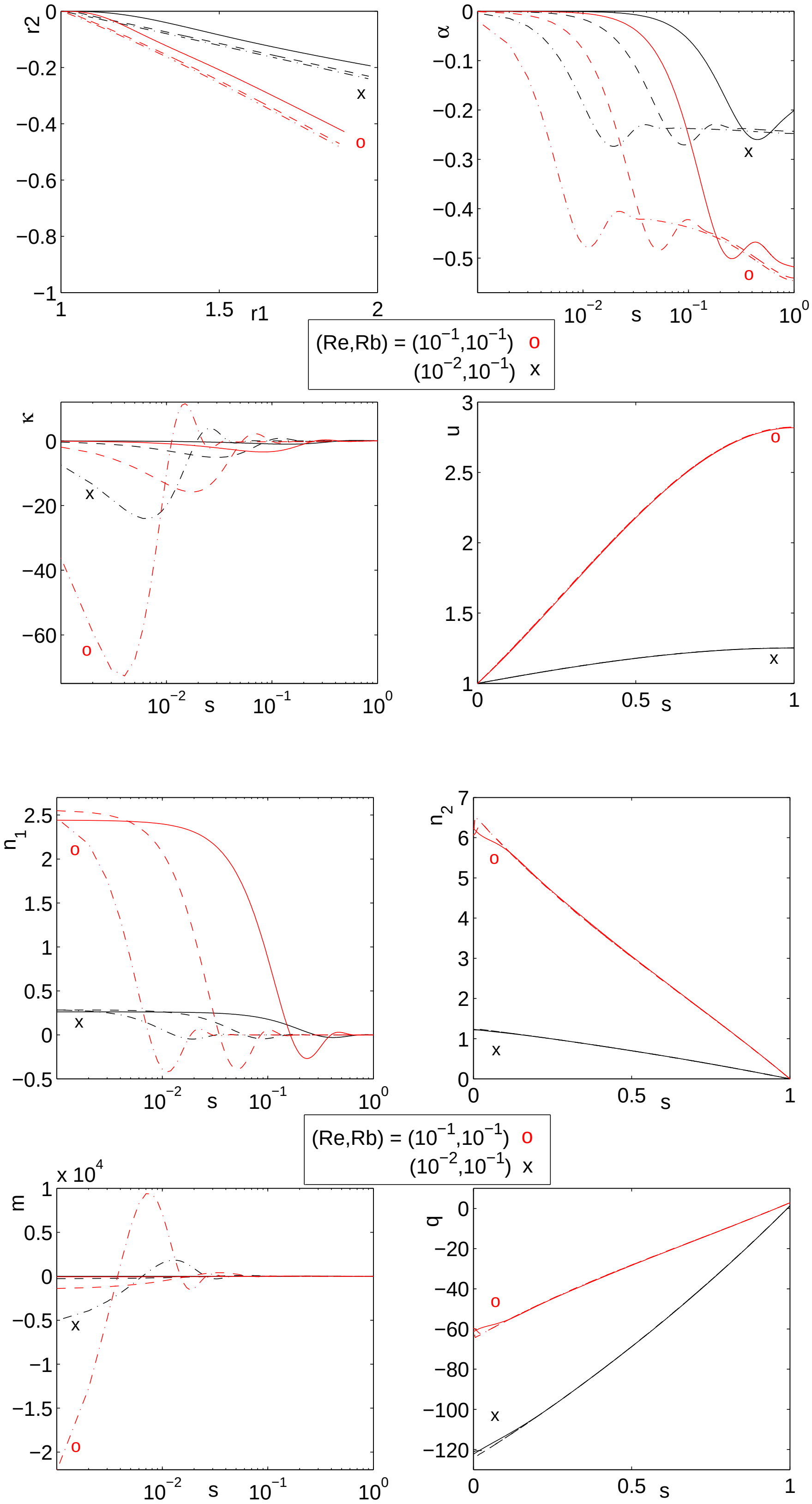

FIGURE 4.5. Viscous-inertial regime. Influence of thickness and viscosity on jet dynamics exposed to rotations of $\mathrm{Rb} = 0.1$: rod solutions with $\epsilon = 10^{-1}, 10^{-2}, 10^{-3}$ are plotted as solid (–), dashed (- -) and dash-dotted (-:) lines, respectively, for $\mathrm{Re} \in \{0.1, 0.01\}$ marked with {o,x}.

Inertial regime: comparison of string and rod model. In the inertial regime for high Reynolds numbers $\{(\mathrm{Re}, \mathrm{Rb}) \,|\, \mathrm{Rb} > \sqrt{3/(2\mathrm{Re})},\ \mathrm{Re} > 10\}$, the dynamics of the jet is unaffected of the thickness ($\epsilon \ll 1$). Already for a moderate slenderness $\epsilon = 10^{-2}$, the rod solution coincides well with the string solution, as figure 4.3 shows. Consequently, the curling behavior at the nozzle is here exclusively determined by rotation and viscosity. The faster the rotation (smaller Rb), the stronger is certainly the bending of the jet and hence the higher is the amplitude of curvature κ, internal shear force n_1 and couple m. In the string associated quantities we observe a steeper descent of the angle α, a higher traction force n_2 and a faster increase and higher velocity u implying smaller cross-sections. The jet is stronger pressed out off the nozzle due to higher centrifugal and Coriolis forces. The influence of the viscosity on the bending is less relevant, but, however, the jet is straighter and faster for higher Re, see figures 4.3, 4.4 and numerical studies of string model in [10].

For low Reynolds numbers, the slenderness ratio additionally affects the jet behavior, as exemplified for $(\mathrm{Re}, \mathrm{Rb}) = (0.01, 1)$ in figure 4.4. The thinner the jet (smaller ϵ), the stronger is the bending κ and the slower is the velocity u. The amplitude of the internal couple m is respectively higher at the nozzle, whereas the shear n_1 and traction forces n_2 are of similar magnitude. The rod solution converges to the string solution as $\epsilon \to 0$. However, be aware that the thickest jet in the example (figure 4.4) satisfies $q(0; 0.01, 1, 0.1) < 0$ and hence belongs to the other regime by definition.

Viscous-inertial regime: usage of rod model for industrial application. In the viscous-inertial regime which is generally characterized by fast rotations ($\mathrm{Rb} \ll 1$), the jet dynamics shows obviously qualitative differences to the results in the inertial regime. For example the jet becomes straighter and slower for smaller Re, see figure 4.5. Moreover, the high rotational forces enforce a strong bending at the nozzle so that a boundary layer arises in angle α, curvature κ, shear force n_2 and couple m. The development of the layer depends on the jet's thickness ϵ and the rotational speed Rb. The thinner the jet (smaller ϵ), the smaller is the layer which implies a higher curvature and internal couple, magnitude of angle and shear force remain unaffected. In particular, the quantities oscillate in the layer, the curvature for example changes from concave to convex and back which is physically very surprising. The faster the rotation (smaller Rb), the more distinct is this behavior, see figure 4.6. More viscous materials (smaller Re) damp the amplitude. Although the observed oscillation is unexpected and negligible on the large scale l of the jet motion, it is by no way numerical nonsense, but has its origin in the model since it is independent of the computational resolution (figure 4.7). To get a deeper insight into the layer without spending higher computational costs, it is worthwhile to transform the system into Lagrangian coordinates. This nonlinear transformation zooms into the nozzle region, see appendix for details. For a theoretical understanding of the boundary layer, a multi-scale analysis might be promising. The existence of

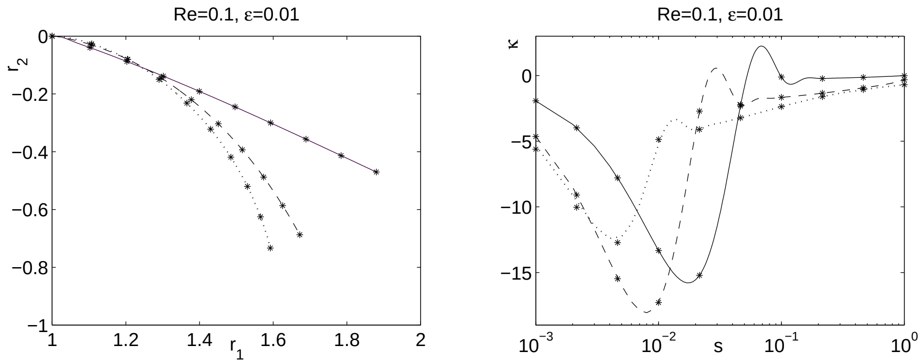

FIGURE 4.6. Viscous-inertial regime. Influence of rotation speed on moderate viscous, slender jet $\mathrm{Re} = 0.1$, $\epsilon = 0.01$: rod dynamics and curvature are plotted for $\mathrm{Rb} \in \{0.1, 0.01, 0.001\}$ as solid (–), dashed (- -), dotted (:) lines, respectively. Ribe's approach is marked with ($\star$).

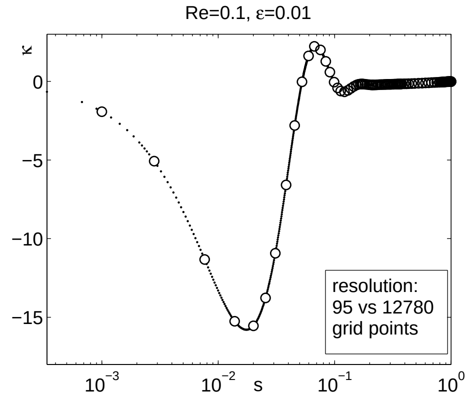

FIGURE 4.7. Different resolution of the boundary layer in κ for $\mathrm{Rb} = 0.1$, cf. figure 4.6.

different scales are already indicated by the inviscid string solution for the velocity $u(s) = \sqrt{2s}/\mathrm{Rb}$ with $u(0) = 0 \neq 1$ for all Rb. But this remains to future research.

At last, note that the numerical solvability of the rod model in this regime depends crucially on the regularizing effect of the slenderness parameter ϵ. If ϵ is chosen too small ($\epsilon \approx 0$), the rod model turns numerically into the string model and the arising huge gradients at the nozzle cause numerical failures.

Remark 9. *In spite of the different approximations of the incompressibility, the numerical results of our rod model and Ribe's approach coincide for all parameter ranges* $(\mathrm{Re}, \mathrm{Rb}, \epsilon)$*. This confirms the asymptotic consideration in remark 6 and justifies the omission of the offset field in* (2.1)*, i.e.* $\mathbf{c} = \mathbf{0}$.

5. Conclusion

Studying the curling behavior of viscous jets in rotational spinning processes in this paper, we have developed a consistent, instationary Cosserat rod model based on an incompressible geometrical model and appropriate material laws in the context of slender-body theory. The rod model differs from Ribe's approach [17] in the approximation of incompressibility which turns out to have no effect on the numerical solution. Moreover, it reduces to the string model of [12] in the limit $\epsilon \to 0$ implying the absence of shear forces. The numerical analysis of the representative, stationary two-dimensional set-up where the jet dynamics depends on viscosity and rotation reveals that the rod model not only covers the string model in the inertia-dominated jet regime but also overcomes its limitations [10] and enables the numerical handling of the viscous-inertial jet regime. Thus, the rod model shows its applicability for the simulation and optimization of jets with certain thickness ϵ and industrially relevant parameters $(\mathrm{Re}, \mathrm{Rb})$.

However, with a view towards the simulation of the instationary three-dimensional rotational spinning processes in industrial applications, an efficient numerical treatment of the free boundary value problem of partial differential equations (3.1) is required. Therefore, the consideration of the Lagrangian framework and a multi-scale analysis could be helpful. Future extensions might moreover include the incorporation of temperature dependence and aerodynamic forces in the rod model.

Acknowledgements. This work has been supported by Rheinland-Pfalz Excellence Center for Mathematical and Computational Modeling $(\mathrm{CM})^2$.

Appendix

In view of an analysis of the boundary layer at the nozzle for $\mathrm{Rb} \to 0$, it might be suitable to consider our stationary Eulerian rod model (3.4) in its associated Lagrangian form. The stationarity simplifies the transformation between Eulerian and Lagrangian coordinates (cf. section 2.2) to

$$\partial_t S(\sigma,t) = \tilde{u}(S(\sigma,t)), \qquad S(\sigma, t_{in}(\sigma)) = 0,$$

where $t_{in}(\sigma)$ prescribes the time of the material point σ entering the steady flow domain $S(\sigma,t) \in [0,l]$. Thus, $S(\sigma,t) = \hat{S}(t - t_{in}(\sigma))$ holds. This exclusive dependence on the run time $\zeta = t - t_{in}(\sigma)$ of the material point is also valid for all other fields, $f(\sigma,t) = \hat{f}(t - t_{in}(\sigma))$. Determining the material coordinates via $t_{in}(\sigma) = -\sigma/u_0$, we have $\partial_t f(\sigma,t) = u_0 \partial_\sigma f(\sigma,t) = \partial_\zeta \hat{f}(t + \sigma/u_0)$. Consequently, $u = \partial_t S = u_0 \partial_\sigma S = u_0 e$ in the Lagrangian setting, and the convective velocity and the strain coincide because $u_0 = 1$ in the dimensionless form. Using calculus 5 and dropping $\hat{\ }$, the Lagrangian rod model reads

$$\begin{aligned}
&\partial_\zeta \check{\mathfrak{r}} = e\chi(\alpha), && \check{\mathfrak{r}}(0) = (1,0)\\
&\partial_\zeta \alpha = \kappa, && \alpha(0) = 0\\
&\partial_\zeta \kappa = \frac{4}{3} e^3 m, && \kappa(0) = 0\\
&\partial_\zeta e = \frac{1}{3} e^2 n_2, && e(0) = 1\\
&\partial_\zeta n_1 = \kappa n_2 - \mathrm{Re}\kappa e + \frac{\mathrm{Re}}{\mathrm{Rb}^2} \check{\mathfrak{r}} \cdot \chi(\alpha)^\perp - \frac{2\mathrm{Re}}{\mathrm{Rb}} e, && n_1(T) = 0\\
&\partial_\zeta n_2 = \frac{\mathrm{Re}}{3} e^2 n_2 - \kappa n_1 - \frac{\mathrm{Re}}{\mathrm{Rb}^2} \check{\mathfrak{r}} \cdot \chi(\alpha), && n_2(T) = 0\\
&\partial_\zeta m = \frac{\mathrm{Re}}{3} e^2 m + \frac{4}{\epsilon^2} e n_1 - \frac{\mathrm{Re}}{12\mathrm{Rb}} n_2 - \frac{\mathrm{Re}}{12} \kappa n_2 && m(T) = 0.
\end{aligned}$$

The nonlinear transformation between Eulerian and Lagrangian coordinates allows to zoom into the nozzle region while keeping the same number of discretization points, as visualized in figure 5.8.

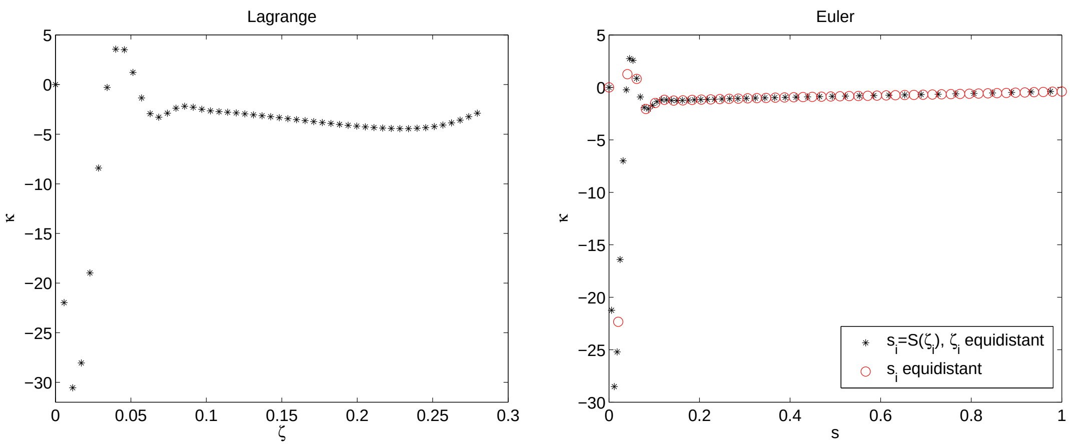

FIGURE 5.8. Resolution of boundary layer in κ for $(\mathrm{Re}, \mathrm{Rb}, \epsilon) = (1, 0.1, 0.01)$. Left: Lagrangian setting, 50 equidistant grid points ζ_i. Right: Eulerian setting, transformed grid points $\hat{S}(\zeta_i)$ ($\star$) versus 50 equidistant arc-lengths s_i ($\circ$).

REFERENCES

[1] S. S. ANTMAN, *Nonlinear Problems of Elasticity*, Springer Verlag, New York, 2006.

[2] S. CHIU-WEBSTER AND J. R. LISTER, *The fall of a viscous thread onto a moving surface: A 'fluid-mechanical sewing machine'*, J. Fluid. Mech., 569 (2006), pp. 89–111.

[3] L. J. CUMMINGS AND P. D. HOWELL, *On the evolution of non-axissymetric viscous fibres with surface tension inertia and gravity*, J. Fluid. Mech., 389 (1999), pp. 361–389.

[4] S. P. DECENT, A. C. KING, AND I. M. WALLWORK, *Free jets spun from a prilling tower*, J. Eng. Math., 42 (2002), pp. 265–282.

[5] J. N. Dewynne, P. D. Howell, and P. Wilmott, *Slender viscous fibers with inertia and gravity*, Quart. J. Mech. Appl. Math., 47 (1994), pp. 541–555.
[6] J. N. Dewynne, J. R. Ockendon, and P. Wilmott, *A systematic derivation of the leading-order equations for extensional flows in slender geometries*, J. Fluid. Mech., 244 (1992), pp. 323–338.
[7] J. Eggers and T. Dupont, *Drop formation in a one-dimensional approximation of the Navier-Stokes equation*, J. Fluid. Mech., 262 (2001), pp. 205–221.
[8] V. M. Entov and A. L. Yarin, *The dynamics of thin liquid jets in air*, J. Fluid. Mech., 140 (1984), pp. 91–111.
[9] D. S. Finnicum, S. J. Weinstein, and K. J. Ruschak, *The effect of applied pressure on the shape of a two-dimensional liquid curtain falling under the influence of gravity*, J. Fluid. Mech., 255 (1993), pp. 647–665.
[10] T. Götz, A. Klar, A. Unterreiter, and R. Wegener, *Numerical evidence for the non-existence of solutions to the equations describing rotational fiber spinning*, Math. Mod. Meth. Appl. Sci., 18 (2008), pp. 1829–1844.
[11] A. Hlod, *Curved jets of viscous fluid: interactions with a moving wall*, PhD thesis, Eindhoven University of Technology, 2009.
[12] N. Marheineke and R. Wegener, *Asymptotic model for the dynamics of curved viscous fibers with surface tension*, J. Fluid. Mech., 622 (2009), pp. 345–369.
[13] S. Panda, N. Marheineke, and R. Wegener, *Systematic derivation of an asymptotic model for the dynamics of curved viscous fibers*, Math. Meth. Appl. Sci., 31 (2008), pp. 1153–1173.
[14] L. Partridge, D. C. Y. Wong, M. J. H. Simmons, E. I. Parau, and S. P. Decent, *Experimental and theoretical description of the break up of curved liquid jets in the prilling process*, Chem Eng Res Des, 83 (2005), pp. 1267–1275.
[15] J. R. A. Pearson, *Mechanics of polymer processing*, Elsevier, 1985.
[16] N. M. Ribe, *Coiling of viscous jets*, Proc. Roy. Soc. London, A, 2051 (2004), pp. 3223–3239.
[17] N. M. Ribe, M. Habibi, and D. Bonn, *Stability of liquid rope coiling*, Phys. Fluids, 18 (2006), p. 084102.
[18] N. M. Ribe, J. R. Lister, and S. Chiu-Webster, *Stability of a dragged viscous thread: Onset of 'stitching' in a fluid-mechanical 'sewing machine'*, Phys. Fluids, 18 (2006), p. 124105.
[19] I. M. Wallwork, S. P. Decent, A. C. King, and R. M. S. M. Schulkes, *The trajectory and stability of a spiralling liquid jet. Part 1. Inviscid theory*, J. Fluid. Mech., 459 (2002), pp. 43–65.
[20] D. C. Y. Wong, M. J. H. Simmons, S. P. Decent, E. I. Parau, and A. C. King, *Break up dynamics and drop size distributions created from curved liquid jets*, Int. J. Multiphase Flow, 30 (2004), pp. 499–520.
[21] A. L. Yarin, *Free liquid jets and films: Hydrodynamics and rheology*, Longman, New York, 1993.

W. Arne, Universität Kassel, Fachbereich Mathematik, Kassel, Germany
E-mail address: walter_ada@web.de

N. Marheineke, Johannes-Gutenberg Universität Mainz, Institut für Mathematik, Mainz, Germany
E-mail address: marheineke@mathematik.uni-kl.de

A. Meister, Universität Kassel, Fachbereich Mathematik, Kassel, Germany
E-mail address: meister@mathematik.uni-kassel.de

R. Wegener, Fraunhofer ITWM, Kaiserslautern, Germany
E-mail address: wegener@itwm.fhg.de

Published reports of the Fraunhofer ITWM

The PDF-files of the following reports are available under:
www.itwm.fraunhofer.de/de/ zentral__berichte/berichte

1. D. Hietel, K. Steiner, J. Struckmeier
A Finite - Volume Particle Method for Compressible Flows
(19 pages, 1998)

2. M. Feldmann, S. Seibold
Damage Diagnosis of Rotors: Application of Hilbert Transform and Multi-Hypothesis Testing
Keywords: Hilbert transform, damage diagnosis, Kalman filtering, non-linear dynamics
(23 pages, 1998)

3. Y. Ben-Haim, S. Seibold
Robust Reliability of Diagnostic Multi-Hypothesis Algorithms: Application to Rotating Machinery
Keywords: Robust reliability, convex models, Kalman filtering, multi-hypothesis diagnosis, rotating machinery, crack diagnosis
(24 pages, 1998)

4. F.-Th. Lentes, N. Siedow
Three-dimensional Radiative Heat Transfer in Glass Cooling Processes
(23 pages, 1998)

5. A. Klar, R. Wegener
A hierarchy of models for multilane vehicular traffic
Part I: Modeling
(23 pages, 1998)

Part II: Numerical and stochastic investigations
(17 pages, 1998)

6. A. Klar, N. Siedow
Boundary Layers and Domain Decomposition for Radiative Heat Transfer and Diffusion Equations: Applications to Glass Manufacturing Processes
(24 pages, 1998)

7. I. Choquet
Heterogeneous catalysis modelling and numerical simulation in rarified gas flows
Part I: Coverage locally at equilibrium
(24 pages, 1998)

8. J. Ohser, B. Steinbach, C. Lang
Efficient Texture Analysis of Binary Images
(17 pages, 1998)

9. J. Orlik
Homogenization for viscoelasticity of the integral type with aging and shrinkage
(20 pages, 1998)

10. J. Mohring
Helmholtz Resonators with Large Aperture
(21 pages, 1998)

11. H. W. Hamacher, A. Schöbel
On Center Cycles in Grid Graphs
(15 pages, 1998)

12. H. W. Hamacher, K.-H. Küfer
Inverse radiation therapy planning - a multiple objective optimisation approach
(14 pages, 1999)

13. C. Lang, J. Ohser, R. Hilfer
On the Analysis of Spatial Binary Images
(20 pages, 1999)

14. M. Junk
On the Construction of Discrete Equilibrium Distributions for Kinetic Schemes
(24 pages, 1999)

15. M. Junk, S. V. Raghurame Rao
A new discrete velocity method for Navier-Stokes equations
(20 pages, 1999)

16. H. Neunzert
Mathematics as a Key to Key Technologies
(39 pages (4 PDF-Files), 1999)

17. J. Ohser, K. Sandau
Considerations about the Estimation of the Size Distribution in Wicksell's Corpuscle Problem
(18 pages, 1999)

18. E. Carrizosa, H. W. Hamacher, R. Klein, S. Nickel
Solving nonconvex planar location problems by finite dominating sets
Keywords: Continuous Location, Polyhedral Gauges, Finite Dominating Sets, Approximation, Sandwich Algorithm, Greedy Algorithm
(19 pages, 2000)

19. A. Becker
A Review on Image Distortion Measures
Keywords: Distortion measure, human visual system
(26 pages, 2000)

20. H. W. Hamacher, M. Labbé, S. Nickel, T. Sonneborn
Polyhedral Properties of the Uncapacitated Multiple Allocation Hub Location Problem
Keywords: integer programming, hub location, facility location, valid inequalities, facets, branch and cut
(21 pages, 2000)

21. H. W. Hamacher, A. Schöbel
Design of Zone Tariff Systems in Public Transportation
(30 pages, 2001)

22. D. Hietel, M. Junk, R. Keck, D. Teleaga
The Finite-Volume-Particle Method for Conservation Laws
(16 pages, 2001)

23. T. Bender, H. Hennes, J. Kalcsics, M. T. Melo, S. Nickel
Location Software and Interface with GIS and Supply Chain Management
Keywords: facility location, software development, geographical information systems, supply chain management
(48 pages, 2001)

24. H. W. Hamacher, S. A. Tjandra
Mathematical Modelling of Evacuation Problems: A State of Art
(44 pages, 2001)

25. J. Kuhnert, S. Tiwari
Grid free method for solving the Poisson equation
Keywords: Poisson equation, Least squares method, Grid free method
(19 pages, 2001)

26. T. Götz, H. Rave, D. Reinel-Bitzer, K. Steiner, H. Tiemeier
Simulation of the fiber spinning process
Keywords: Melt spinning, fiber model, Lattice Boltzmann, CFD
(19 pages, 2001)

27. A. Zemitis
On interaction of a liquid film with an obstacle
Keywords: impinging jets, liquid film, models, numerical solution, shape
(22 pages, 2001)

28. I. Ginzburg, K. Steiner
Free surface lattice-Boltzmann method to model the filling of expanding cavities by Bingham Fluids
Keywords: Generalized LBE, free-surface phenomena, interface boundary conditions, filling processes, Bingham viscoplastic model, regularized models
(22 pages, 2001)

29. H. Neunzert
»Denn nichts ist für den Menschen als Menschen etwas wert, was er nicht mit Leidenschaft tun kann«
Vortrag anlässlich der Verleihung des Akademiepreises des Landes Rheinland-Pfalz am 21.11.2001
Keywords: Lehre, Forschung, angewandte Mathematik, Mehrskalenanalyse, Strömungsmechanik
(18 pages, 2001)

30. J. Kuhnert, S. Tiwari
Finite pointset method based on the projection method for simulations of the incompressible Navier-Stokes equations
Keywords: Incompressible Navier-Stokes equations, Meshfree method, Projection method, Particle scheme, Least squares approximation
AMS subject classification: 76D05, 76M28
(25 pages, 2001)

31. R. Korn, M. Krekel
Optimal Portfolios with Fixed Consumption or Income Streams
Keywords: Portfolio optimisation, stochastic control, HJB equation, discretisation of control problems
(23 pages, 2002)

32. M. Krekel
Optimal portfolios with a loan dependent credit spread
Keywords: Portfolio optimisation, stochastic control, HJB equation, credit spread, log utility, power utility, non-linear wealth dynamics
(25 pages, 2002)

33. J. Ohser, W. Nagel, K. Schladitz
The Euler number of discretized sets – on the choice of adjacency in homogeneous lattices
Keywords: image analysis, Euler number, neighborhod relationships, cuboidal lattice
(32 pages, 2002)

34. I. Ginzburg, K. Steiner
Lattice Boltzmann Model for Free-Surface flow and Its Application to Filling Process in Casting
Keywords: Lattice Boltzmann models; free-surface phenomena; interface boundary conditions; filling processes; injection molding; volume of fluid method; interface boundary conditions; advection-schemes; upwind-schemes
(54 pages, 2002)

35. M. Günther, A. Klar, T. Materne, R. Wegener
Multivalued fundamental diagrams and stop and go waves for continuum traffic equations
Keywords: traffic flow, macroscopic equations, kinetic derivation, multivalued fundamental diagram, stop and go waves, phase transitions
(25 pages, 2002)

36. S. Feldmann, P. Lang, D. Prätzel-Wolters
Parameter influence on the zeros of network determinants
Keywords: Networks, Equicofactor matrix polynomials, Realization theory, Matrix perturbation theory
(30 pages, 2002)

37. K. Koch, J. Ohser, K. Schladitz
Spectral theory for random closed sets and estimating the covariance via frequency space
Keywords: Random set, Bartlett spectrum, fast Fourier transform, power spectrum
(28 pages, 2002)

38. D. d'Humières, I. Ginzburg
Multi-reflection boundary conditions for lattice Boltzmann models
Keywords: lattice Boltzmann equation, boudary condistions, bounce-back rule, Navier-Stokes equation
(72 pages, 2002)

39. R. Korn
Elementare Finanzmathematik
Keywords: Finanzmathematik, Aktien, Optionen, Portfolio-Optimierung, Börse, Lehrerweiterbildung, Mathematikunterricht
(98 pages, 2002)

40. J. Kallrath, M. C. Müller, S. Nickel
Batch Presorting Problems: Models and Complexity Results
Keywords: Complexity theory, Integer programming, Assigment, Logistics
(19 pages, 2002)

41. J. Linn
On the frame-invariant description of the phase space of the Folgar-Tucker equation
Key words: fiber orientation, Folgar-Tucker equation, injection molding
(5 pages, 2003)

42. T. Hanne, S. Nickel
A Multi-Objective Evolutionary Algorithm for Scheduling and Inspection Planning in Software Development Projects
Key words: multiple objective programming, project management and scheduling, software development, evolutionary algorithms, efficient set
(29 pages, 2003)

43. T. Bortfeld , K.-H. Küfer, M. Monz, A. Scherrer, C. Thieke, H. Trinkaus
Intensity-Modulated Radiotherapy - A Large Scale Multi-Criteria Programming Problem
Keywords: multiple criteria optimization, representative systems of Pareto solutions, adaptive triangulation, clustering and disaggregation techniques, visualization of Pareto solutions, medical physics, external beam radiotherapy planning, intensity modulated radiotherapy
(31 pages, 2003)

44. T. Halfmann, T. Wichmann
Overview of Symbolic Methods in Industrial Analog Circuit Design
Keywords: CAD, automated analog circuit design, symbolic analysis, computer algebra, behavioral modeling, system simulation, circuit sizing, macro modeling, differential-algebraic equations, index
(17 pages, 2003)

45. S. E. Mikhailov, J. Orlik
Asymptotic Homogenisation in Strength and Fatigue Durability Analysis of Composites
Keywords: multiscale structures, asymptotic homogenization, strength, fatigue, singularity, non-local conditions
(14 pages, 2003)

46. P. Domínguez-Marín, P. Hansen, N. Mladenovi´c , S. Nickel
Heuristic Procedures for Solving the Discrete Ordered Median Problem
Keywords: genetic algorithms, variable neighborhood search, discrete facility location
(31 pages, 2003)

47. N. Boland, P. Domínguez-Marín, S. Nickel, J. Puerto
Exact Procedures for Solving the Discrete Ordered Median Problem
Keywords: discrete location, Integer programming
(41 pages, 2003)

48. S. Feldmann, P. Lang
Padé-like reduction of stable discrete linear systems preserving their stability
Keywords: Discrete linear systems, model reduction, stability, Hankel matrix, Stein equation
(16 pages, 2003)

49. J. Kallrath, S. Nickel
A Polynomial Case of the Batch Presorting Problem
Keywords: batch presorting problem, online optimization, competetive analysis, polynomial algorithms, logistics
(17 pages, 2003)

50. T. Hanne, H. L. Trinkaus
knowCube for MCDM – Visual and Interactive Support for Multicriteria Decision Making
Key words: Multicriteria decision making, knowledge management, decision support systems, visual interfaces, interactive navigation, real-life applications.
(26 pages, 2003)

51. O. Iliev, V. Laptev
On Numerical Simulation of Flow Through Oil Filters
Keywords: oil filters, coupled flow in plain and porous media, Navier-Stokes, Brinkman, numerical simulation
(8 pages, 2003)

52. W. Dörfler, O. Iliev, D. Stoyanov, D. Vassileva
On a Multigrid Adaptive Refinement Solver for Saturated Non-Newtonian Flow in Porous Media
Keywords: Nonlinear multigrid, adaptive refinement, non-Newtonian flow in porous media
(17 pages, 2003)

53. S. Kruse
On the Pricing of Forward Starting Options under Stochastic Volatility
Keywords: Option pricing, forward starting options, Heston model, stochastic volatility, cliquet options
(11 pages, 2003)

54. O. Iliev, D. Stoyanov
Multigrid – adaptive local refinement solver for incompressible flows
Keywords: Navier-Stokes equations, incompressible flow, projection-type splitting, SIMPLE, multigrid methods, adaptive local refinement, lid-driven flow in a cavity
(37 pages, 2003)

55. V. Starikovicius
The multiphase flow and heat transfer in porous media
Keywords: Two-phase flow in porous media, various formulations, global pressure, multiphase mixture model, numerical simulation
(30 pages, 2003)

56. P. Lang, A. Sarishvili, A. Wirsen
Blocked neural networks for knowledge extraction in the software development process
Keywords: Blocked Neural Networks, Nonlinear Regression, Knowledge Extraction, Code Inspection
(21 pages, 2003)

57. H. Knaf, P. Lang, S. Zeiser
Diagnosis aiding in Regulation Thermography using Fuzzy Logic
Keywords: fuzzy logic,knowledge representation, expert system
(22 pages, 2003)

58. M. T. Melo, S. Nickel, F. Saldanha da Gama
Largescale models for dynamic multicommodity capacitated facility location
Keywords: supply chain management, strategic planning, dynamic location, modeling
(40 pages, 2003)

59. J. Orlik
Homogenization for contact problems with periodically rough surfaces
Keywords: asymptotic homogenization, contact problems
(28 pages, 2004)

60. A. Scherrer, K.-H. Küfer, M. Monz, F. Alonso, T. Bortfeld
IMRT planning on adaptive volume structures – a significant advance of computational complexity
Keywords: Intensity-modulated radiation therapy (IMRT), inverse treatment planning, adaptive volume structures, hierarchical clustering, local refinement, adaptive clustering, convex programming, mesh generation, multi-grid methods
(24 pages, 2004)

61. D. Kehrwald
Parallel lattice Boltzmann simulation of complex flows
Keywords: Lattice Boltzmann methods, parallel computing, microstructure simulation, virtual material design, pseudo-plastic fluids, liquid composite moulding
(12 pages, 2004)

62. O. Iliev, J. Linn, M. Moog, D. Niedziela, V. Starikovicius
On the Performance of Certain Iterative Solvers for Coupled Systems Arising in Discretization of Non-Newtonian Flow Equations

Keywords: Performance of iterative solvers, Preconditioners, Non-Newtonian flow
(17 pages, 2004)

63. R. Ciegis, O. Iliev, S. Rief, K. Steiner
On Modelling and Simulation of Different Regimes for Liquid Polymer Moulding
Keywords: Liquid Polymer Moulding, Modelling, Simulation, Infiltration, Front Propagation, non-Newtonian flow in porous media
(43 pages, 2004)

64. T. Hanne, H. Neu
Simulating Human Resources in Software Development Processes
Keywords: Human resource modeling, software process, productivity, human factors, learning curve
(14 pages, 2004)

65. O. Iliev, A. Mikelic, P. Popov
Fluid structure interaction problems in deformable porous media: Toward permeability of deformable porous media
Keywords: fluid-structure interaction, deformable porous media, upscaling, linear elasticity, stokes, finite elements
(28 pages, 2004)

66. F. Gaspar, O. Iliev, F. Lisbona, A. Naumovich, P. Vabishchevich
On numerical solution of 1-D poroelasticity equations in a multilayered domain
Keywords: poroelasticity, multilayered material, finite volume discretization, MAC type grid
(41 pages, 2004)

67. J. Ohser, K. Schladitz, K. Koch, M. Nöthe
Diffraction by image processing and its application in materials science
Keywords: porous microstructure, image analysis, random set, fast Fourier transform, power spectrum, Bartlett spectrum
(13 pages, 2004)

68. H. Neunzert
Mathematics as a Technology: Challenges for the next 10 Years
Keywords: applied mathematics, technology, modelling, simulation, visualization, optimization, glass processing, spinning processes, fiber-fluid interaction, trubulence effects, topological optimization, multicriteria optimization, Uncertainty and Risk, financial mathematics, Malliavin calculus, Monte-Carlo methods, virtual material design, filtration, bio-informatics, system biology
(29 pages, 2004)

69. R. Ewing, O. Iliev, R. Lazarov, A. Naumovich
On convergence of certain finite difference discretizations for 1D poroelasticity interface problems
Keywords: poroelasticity, multilayered material, finite volume discretizations, MAC type grid, error estimates
(26 pages,2004)

70. W. Dörfler, O. Iliev, D. Stoyanov, D. Vassileva
On Efficient Simulation of Non-Newtonian Flow in Saturated Porous Media with a Multigrid Adaptive Refinement Solver
Keywords: Nonlinear multigrid, adaptive renement, non-Newtonian in porous media
(25 pages, 2004)

71. J. Kalcsics, S. Nickel, M. Schröder
Towards a Unified Territory Design Approach – Applications, Algorithms and GIS Integration
Keywords: territory desgin, political districting, sales territory alignment, optimization algorithms, Geographical Information Systems
(40 pages, 2005)

72. K. Schladitz, S. Peters, D. Reinel-Bitzer, A. Wiegmann, J. Ohser
Design of acoustic trim based on geometric modeling and flow simulation for non-woven
Keywords: random system of fibers, Poisson line process, flow resistivity, acoustic absorption, Lattice-Boltzmann method, non-woven
(21 pages, 2005)

73. V. Rutka, A. Wiegmann
Explicit Jump Immersed Interface Method for virtual material design of the effective elastic moduli of composite materials
Keywords: virtual material design, explicit jump immersed interface method, effective elastic moduli, composite materials
(22 pages, 2005)

74. T. Hanne
Eine Übersicht zum Scheduling von Baustellen
Keywords: Projektplanung, Scheduling, Bauplanung, Bauindustrie
(32 pages, 2005)

75. J. Linn
The Folgar-Tucker Model as a Differetial Algebraic System for Fiber Orientation Calculation
Keywords: fiber orientation, Folgar–Tucker model, invariants, algebraic constraints, phase space, trace stability
(15 pages, 2005)

76. M. Speckert, K. Dreßler, H. Mauch, A. Lion, G. J. Wierda
Simulation eines neuartigen Prüfsystems für Achserprobungen durch MKS-Modellierung einschließlich Regelung
Keywords: virtual test rig, suspension testing, multibody simulation, modeling hexapod test rig, optimization of test rig configuration
(20 pages, 2005)

77. K.-H. Küfer, M. Monz, A. Scherrer, P. Süss, F. Alonso, A.S.A. Sultan, Th. Bortfeld, D. Craft, Chr. Thieke
Multicriteria optimization in intensity modulated radiotherapy planning
Keywords: multicriteria optimization, extreme solutions, real-time decision making, adaptive approximation schemes, clustering methods, IMRT planning, reverse engineering
(51 pages, 2005)

78. S. Amstutz, H. Andrä
A new algorithm for topology optimization using a level-set method
Keywords: shape optimization, topology optimization, topological sensitivity, level-set
(22 pages, 2005)

79. N. Ettrich
Generation of surface elevation models for urban drainage simulation
Keywords: Flooding, simulation, urban elevation models, laser scanning
(22 pages, 2005)

80. H. Andrä, J. Linn, I. Matei, I. Shklyar, K. Steiner, E. Teichmann
OPTCAST – Entwicklung adäquater Strukturoptimierungsverfahren für Gießereien Technischer Bericht (KURZFASSUNG)
Keywords: Topologieoptimierung, Level-Set-Methode, Gießprozesssimulation, Gießtechnische Restriktionen, CAE-Kette zur Strukturoptimierung
(77 pages, 2005)

81. N. Marheineke, R. Wegener
Fiber Dynamics in Turbulent Flows Part I: General Modeling Framework
Keywords: fiber-fluid interaction; Cosserat rod; turbulence modeling; Kolmogorov's energy spectrum; double-velocity correlations; differentiable Gaussian fields
(20 pages, 2005)

Part II: Specific Taylor Drag
Keywords: flexible fibers; k-ε turbulence model; fiber-turbulence interaction scales; air drag; random Gaussian aerodynamic force; white noise; stochastic differential equations; ARMA process
(18 pages, 2005)

82. C. H. Lampert, O. Wirjadi
An Optimal Non-Orthogonal Separation of the Anisotropic Gaussian Convolution Filter
Keywords: Anisotropic Gaussian filter, linear filtering, orientation space, nD image processing, separable filters
(25 pages, 2005)

83. H. Andrä, D. Stoyanov
Error indicators in the parallel finite element solver for linear elasticity DDFEM
Keywords: linear elasticity, finite element method, hierarchical shape functions, domain decom-position, parallel implementation, a posteriori error estimates
(21 pages, 2006)

84. M. Schröder, I. Solchenbach
Optimization of Transfer Quality in Regional Public Transit
Keywords: public transit, transfer quality, quadratic assignment problem
(16 pages, 2006)

85. A. Naumovich, F. J. Gaspar
On a multigrid solver for the three-dimensional Biot poroelasticity system in multilayered domains
Keywords: poroelasticity, interface problem, multigrid, operator-dependent prolongation
(11 pages, 2006)

86. S. Panda, R. Wegener, N. Marheineke
Slender Body Theory for the Dynamics of Curved Viscous Fibers
Keywords: curved viscous fibers; fluid dynamics; Navier-Stokes equations; free boundary value problem; asymptotic expansions; slender body theory
(14 pages, 2006)

87. E. Ivanov, H. Andrä, A. Kudryavtsev
Domain Decomposition Approach for Automatic Parallel Generation of Tetrahedral Grids
Key words: Grid Generation, Unstructured Grid, Delaunay Triangulation, Parallel Programming, Domain Decomposition, Load Balancing
(18 pages, 2006)

88. S. Tiwari, S. Antonov, D. Hietel, J. Kuhnert, R. Wegener
A Meshfree Method for Simulations of Interactions between Fluids and Flexible Structures
Key words: Meshfree Method, FPM, Fluid Structure Interaction, Sheet of Paper, Dynamical Coupling
(16 pages, 2006)

89. R. Ciegis , O. Iliev, V. Starikovicius, K. Steiner
Numerical Algorithms for Solving Problems of Multiphase Flows in Porous Media
Keywords: nonlinear algorithms, finite-volume method, software tools, porous media, flows
(16 pages, 2006)

90. D. Niedziela, O. Iliev, A. Latz
On 3D Numerical Simulations of Viscoelastic Fluids
Keywords: non-Newtonian fluids, anisotropic viscosity, integral constitutive equation
(18 pages, 2006)

91. A. Winterfeld
Application of general semi-infinite Programming to Lapidary Cutting Problems
Keywords: large scale optimization, nonlinear programming, general semi-infinite optimization, design centering, clustering
(26 pages, 2006)

92. J. Orlik, A. Ostrovska
Space-Time Finite Element Approximation and Numerical Solution of Hereditary Linear Viscoelasticity Problems
Keywords: hereditary viscoelasticity; kern approximation by interpolation; space-time finite element approximation, stability and a priori estimate
(24 pages, 2006)

93. V. Rutka, A. Wiegmann, H. Andrä
EJIIM for Calculation of effective Elastic Moduli in 3D Linear Elasticity
Keywords: Elliptic PDE, linear elasticity, irregular domain, finite differences, fast solvers, effective elastic moduli
(24 pages, 2006)

94. A. Wiegmann, A. Zemitis
EJ-HEAT: A Fast Explicit Jump Harmonic Averaging Solver for the Effective Heat Conductivity of Composite Materials
Keywords: Stationary heat equation, effective thermal conductivity, explicit jump, discontinuous coefficients, virtual material design, microstructure simulation, EJ-HEAT
(21 pages, 2006)

95. A. Naumovich
On a finite volume discretization of the three-dimensional Biot poroelasticity system in multilayered domains
Keywords: Biot poroelasticity system, interface problems, finite volume discretization, finite difference method
(21 pages, 2006)

96. M. Krekel, J. Wenzel
A unified approach to Credit Default Swaption and Constant Maturity Credit Default Swap valuation
Keywords: LIBOR market model, credit risk, Credit Default Swaption, Constant Maturity Credit Default Swap-method
(43 pages, 2006)

97. A. Dreyer
Interval Methods for Analog Circiuts
Keywords: interval arithmetic, analog circuits, tolerance analysis, parametric linear systems, frequency response, symbolic analysis, CAD, computer algebra
(36 pages, 2006)

98. N. Weigel, S. Weihe, G. Bitsch, K. Dreßler
Usage of Simulation for Design and Optimization of Testing
Keywords: Vehicle test rigs, MBS, control, hydraulics, testing philosophy
(14 pages, 2006)

99. H. Lang, G. Bitsch, K. Dreßler, M. Speckert
Comparison of the solutions of the elastic and elastoplastic boundary value problems
Keywords: Elastic BVP, elastoplastic BVP, variational inequalities, rate-independency, hysteresis, linear kinematic hardening, stop- and play-operator
(21 pages, 2006)

100. M. Speckert, K. Dreßler, H. Mauch
MBS Simulation of a hexapod based suspension test rig
Keywords: Test rig, MBS simulation, suspension, hydraulics, controlling, design optimization
(12 pages, 2006)

101. S. Azizi Sultan, K.-H. Küfer
A dynamic algorithm for beam orientations in multicriteria IMRT planning
Keywords: radiotherapy planning, beam orientation optimization, dynamic approach, evolutionary algorithm, global optimization
(14 pages, 2006)

102. T. Götz, A. Klar, N. Marheineke, R. Wegener
A Stochastic Model for the Fiber Lay-down Process in the Nonwoven Production
Keywords: fiber dynamics, stochastic Hamiltonian system, stochastic averaging
(17 pages, 2006)

103. Ph. Süss, K.-H. Küfer
Balancing control and simplicity: a variable aggregation method in intensity modulated radiation therapy planning
Keywords: IMRT planning, variable aggregation, clustering methods
(22 pages, 2006)

104. A. Beaudry, G. Laporte, T. Melo, S. Nickel
Dynamic transportation of patients in hospitals
Keywords: in-house hospital transportation, dial-a-ride, dynamic mode, tabu search
(37 pages, 2006)

105. Th. Hanne
Applying multiobjective evolutionary algorithms in industrial projects
Keywords: multiobjective evolutionary algorithms, discrete optimization, continuous optimization, electronic circuit design, semi-infinite programming, scheduling
(18 pages, 2006)

106. J. Franke, S. Halim
Wild bootstrap tests for comparing signals and images
Keywords: wild bootstrap test, texture classification, textile quality control, defect detection, kernel estimate, nonparametric regression
(13 pages, 2007)

107. Z. Drezner, S. Nickel
Solving the ordered one-median problem in the plane
Keywords: planar location, global optimization, ordered median, big triangle small triangle method, bounds, numerical experiments
(21 pages, 2007)

108. Th. Götz, A. Klar, A. Unterreiter, R. Wegener
Numerical evidance for the non-existing of solutions of the equations desribing rotational fiber spinning
Keywords: rotational fiber spinning, viscous fibers, boundary value problem, existence of solutions
(11 pages, 2007)

109. Ph. Süss, K.-H. Küfer
Smooth intensity maps and the Bortfeld-Boyer sequencer
Keywords: probabilistic analysis, intensity modulated radiotherapy treatment (IMRT), IMRT plan application, step-and-shoot sequencing
(8 pages, 2007)

110. E. Ivanov, O. Gluchshenko, H. Andrä, A. Kudryavtsev
Parallel software tool for decomposing and meshing of 3d structures
Keywords: a-priori domain decomposition, unstructured grid, Delaunay mesh generation
(14 pages, 2007)

111. O. Iliev, R. Lazarov, J. Willems
Numerical study of two-grid preconditioners for 1d elliptic problems with highly oscillating discontinuous coefficients
Keywords: two-grid algorithm, oscillating coefficients, preconditioner
(20 pages, 2007)

112. L. Bonilla, T. Götz, A. Klar, N. Marheineke, R. Wegener
Hydrodynamic limit of the Fokker-Planck-equation describing fiber lay-down processes
Keywords: stochastic dierential equations, Fokker-Planck equation, asymptotic expansion, Ornstein-Uhlenbeck process
(17 pages, 2007)

113. S. Rief
Modeling and simulation of the pressing section of a paper machine
Keywords: paper machine, computational fluid dynamics, porous media
(41 pages, 2007)

114. R. Ciegis, O. Iliev, Z. Lakdawala
On parallel numerical algorithms for simulating industrial filtration problems
Keywords: Navier-Stokes-Brinkmann equations, finite volume discretization method, SIMPLE, parallel computing, data decomposition method
(24 pages, 2007)

115. N. Marheineke, R. Wegener
Dynamics of curved viscous fibers with surface tension
Keywords: Slender body theory, curved viscous bers with surface tension, free boundary value problem
(25 pages, 2007)

116. S. Feth, J. Franke, M. Speckert
Resampling-Methoden zur mse-Korrektur und Anwendungen in der Betriebsfestigkeit
Keywords: Weibull, Bootstrap, Maximum-Likelihood, Betriebsfestigkeit
(16 pages, 2007)

117. H. Knaf
Kernel Fisher discriminant functions – a concise and rigorous introduction
Keywords: wild bootstrap test, texture classification, textile quality control, defect detection, kernel estimate, nonparametric regression
(30 pages, 2007)

118. O. Iliev, I. Rybak
On numerical upscaling for flows in heterogeneous porous media

Keywords: numerical upscaling, heterogeneous porous media, single phase flow, Darcy's law, multiscale problem, effective permeability, multipoint flux approximation, anisotropy
(17 pages, 2007)

119. O. Iliev, I. Rybak
On approximation property of multipoint flux approximation method
Keywords: Multipoint flux approximation, finite volume method, elliptic equation, discontinuous tensor coefficients, anisotropy
(15 pages, 2007)

120. O. Iliev, I. Rybak, J. Willems
On upscaling heat conductivity for a class of industrial problems
Keywords: Multiscale problems, effective heat conductivity, numerical upscaling, domain decomposition
(21 pages, 2007)

121. R. Ewing, O. Iliev, R. Lazarov, I. Rybak
On two-level preconditioners for flow in porous media
Keywords: Multiscale problem, Darcy's law, single phase flow, anisotropic heterogeneous porous media, numerical upscaling, multigrid, domain decomposition, efficient preconditioner
(18 pages, 2007)

122. M. Brickenstein, A. Dreyer
POLYBORI: A Gröbner basis framework for Boolean polynomials
Keywords: Gröbner basis, formal verification, Boolean polynomials, algebraic cryptoanalysis, satisfiability
(23 pages, 2007)

123. O. Wirjadi
Survey of 3d image segmentation methods
Keywords: image processing, 3d, image segmentation, binarization
(20 pages, 2007)

124. S. Zeytun, A. Gupta
A Comparative Study of the Vasicek and the CIR Model of the Short Rate
Keywords: interest rates, Vasicek model, CIR-model, calibration, parameter estimation
(17 pages, 2007)

125. G. Hanselmann, A. Sarishvili
Heterogeneous redundancy in software quality prediction using a hybrid Bayesian approach
Keywords: reliability prediction, fault prediction, non-homogeneous poisson process, Bayesian model averaging
(17 pages, 2007)

126. V. Maag, M. Berger, A. Winterfeld, K.-H. Küfer
A novel non-linear approach to minimal area rectangular packing
Keywords: rectangular packing, non-overlapping constraints, non-linear optimization, regularization, relaxation
(18 pages, 2007)

127. M. Monz, K.-H. Küfer, T. Bortfeld, C. Thieke
Pareto navigation – systematic multi-criteria-based IMRT treatment plan determination
Keywords: convex, interactive multi-objective optimization, intensity modulated radiotherapy planning
(15 pages, 2007)

128. M. Krause, A. Scherrer
On the role of modeling parameters in IMRT plan optimization
Keywords: intensity-modulated radiotherapy (IMRT), inverse IMRT planning, convex optimization, sensitivity analysis, elasticity, modeling parameters, equivalent uniform dose (EUD)
(18 pages, 2007)

129. A. Wiegmann
Computation of the permeability of porous materials from their microstructure by FFF-Stokes
Keywords: permeability, numerical homogenization, fast Stokes solver
(24 pages, 2007)

130. T. Melo, S. Nickel, F. Saldanha da Gama
Facility Location and Supply Chain Management – A comprehensive review
Keywords: facility location, supply chain management, network design
(54 pages, 2007)

131. T. Hanne, T. Melo, S. Nickel
Bringing robustness to patient flow management through optimized patient transports in hospitals
Keywords: Dial-a-Ride problem, online problem, case study, tabu search, hospital logistics
(23 pages, 2007)

132. R. Ewing, O. Iliev, R. Lazarov, I. Rybak, J. Willems
An efficient approach for upscaling properties of composite materials with high contrast of coefficients
Keywords: effective heat conductivity, permeability of fractured porous media, numerical upscaling, fibrous insulation materials, metal foams
(16 pages, 2008)

133. S. Gelareh, S. Nickel
New approaches to hub location problems in public transport planning
Keywords: integer programming, hub location, transportation, decomposition, heuristic
(25 pages, 2008)

134. G. Thömmes, J. Becker, M. Junk, A. K. Vaikuntam, D. Kehrwald, A. Klar, K. Steiner, A. Wiegmann
A Lattice Boltzmann Method for immiscible multiphase flow simulations using the Level Set Method
Keywords: Lattice Boltzmann method, Level Set method, free surface, multiphase flow
(28 pages, 2008)

135. J. Orlik
Homogenization in elasto-plasticity
Keywords: multiscale structures, asymptotic homogenization, nonlinear energy
(40 pages, 2008)

136. J. Almquist, H. Schmidt, P. Lang, J. Deitmer, M. Jirstrand, D. Prätzel-Wolters, H. Becker
Determination of interaction between MCT1 and CAII via a mathematical and physiological approach
Keywords: mathematical modeling; model reduction; electrophysiology; pH-sensitive microelectrodes; proton antenna
(20 pages, 2008)

137. E. Savenkov, H. Andrä, O. Iliev
An analysis of one regularization approach for solution of pure Neumann problem
Keywords: pure Neumann problem, elasticity, regularization, finite element method, condition number
(27 pages, 2008)

138. O. Berman, J. Kalcsics, D. Krass, S. Nickel
The ordered gradual covering location problem on a network
Keywords: gradual covering, ordered median function, network location
(32 pages, 2008)

139. S. Gelareh, S. Nickel
Multi-period public transport design: A novel model and solution approaches
Keywords: Integer programming, hub location, public transport, multi-period planning, heuristics
(31 pages, 2008)

140. T. Melo, S. Nickel, F. Saldanha-da-Gama
Network design decisions in supply chain planning
Keywords: supply chain design, integer programming models, location models, heuristics
(20 pages, 2008)

141. C. Lautensack, A. Särkkä, J. Freitag, K. Schladitz
Anisotropy analysis of pressed point processes
Keywords: estimation of compression, isotropy test, nearest neighbour distance, orientation analysis, polar ice, Ripley's K function
(35 pages, 2008)

142. O. Iliev, R. Lazarov, J. Willems
A Graph-Laplacian approach for calculating the effective thermal conductivity of complicated fiber geometries
Keywords: graph laplacian, effective heat conductivity, numerical upscaling, fibrous materials
(14 pages, 2008)

143. J. Linn, T. Stephan, J. Carlsson, R. Bohlin
Fast simulation of quasistatic rod deformations for VR applications
Keywords: quasistatic deformations, geometrically exact rod models, variational formulation, energy minimization, finite differences, nonlinear conjugate gradients
(7 pages, 2008)

144. J. Linn, T. Stephan
Simulation of quasistatic deformations using discrete rod models
Keywords: quasistatic deformations, geometrically exact rod models, variational formulation, energy minimization, finite differences, nonlinear conjugate gradients
(9 pages, 2008)

145. J. Marburger, N. Marheineke, R. Pinnau
Adjoint based optimal control using meshless discretizations
Keywords: Mesh-less methods, particle methods, Eulerian-Lagrangian formulation, optimization strategies, adjoint method, hyperbolic equations
(14 pages, 2008

146. S. Desmettre, J. Gould, A. Szimayer
Own-company stockholding and work effort preferences of an unconstrained executive
Keywords: optimal portfolio choice, executive compensation
(33 pages, 2008)

147. M. Berger, M. Schröder, K.-H. Küfer
A constraint programming approach for the two-dimensional rectangular packing problem with orthogonal orientations
Keywords: rectangular packing, orthogonal orientations non-overlapping constraints, constraint propagation
(13 pages, 2008)

148. K. Schladitz, C. Redenbach, T. Sych, M. Godehardt
Microstructural characterisation of open foams using 3d images
Keywords: virtual material design, image analysis, open foams
(30 pages, 2008)

149. E. Fernández, J. Kalcsics, S. Nickel, R. Ríos-Mercado
A novel territory design model arising in the implementation of the WEEE-Directive
Keywords: heuristics, optimization, logistics, recycling
(28 pages, 2008)

150. H. Lang, J. Linn
Lagrangian field theory in space-time for geometrically exact Cosserat rods
Keywords: Cosserat rods, geometrically exact rods, small strain, large deformation, deformable bodies, Lagrangian field theory, variational calculus
(19 pages, 2009)

151. K. Dreßler, M. Speckert, R. Müller, Ch. Weber
Customer loads correlation in truck engineering
Keywords: Customer distribution, safety critical components, quantile estimation, Monte-Carlo methods
(11 pages, 2009)

152. H. Lang, K. Dreßler
An improved multiaxial stress-strain correction model for elastic FE postprocessing
Keywords: Jiang's model of elastoplasticity, stress-strain correction, parameter identification, automatic differentiation, least-squares optimization, Coleman-Li algorithm
(6 pages, 2009)

153. J. Kalcsics, S. Nickel, M. Schröder
A generic geometric approach to territory design and districting
Keywords: Territory design, districting, combinatorial optimization, heuristics, computational geometry
(32 pages, 2009)

154. Th. Fütterer, A. Klar, R. Wegener
An energy conserving numerical scheme for the dynamics of hyperelastic rods
Keywords: Cosserat rod, hyperealstic, energy conservation, finite differences
(16 pages, 2009)

155. A. Wiegmann, L. Cheng, E. Glatt, O. Iliev, S. Rief
Design of pleated filters by computer simulations
Keywords: Solid-gas separation, solid-liquid separation, pleated filter, design, simulation
(21 pages, 2009)

156. A. Klar, N. Marheineke, R. Wegener
Hierarchy of mathematical models for production processes of technical textiles
Keywords: Fiber-fluid interaction, slender-body theory, turbulence modeling, model reduction, stochastic differential equations, Fokker-Planck equation, asymptotic expansions, parameter identification
(21 pages, 2009)

157. E. Glatt, S. Rief, A. Wiegmann, M. Knefel, E. Wegenke
Structure and pressure drop of real and virtual metal wire meshes
Keywords: metal wire mesh, structure simulation, model calibration, CFD simulation, pressure loss
(7 pages, 2009)

158. S. Kruse, M. Müller
Pricing American call options under the assumption of stochastic dividends – An application of the Korn-Rogers model
Keywords: option pricing, American options, dividends, dividend discount model, Black-Scholes model
(22 pages, 2009)

159. H. Lang, J. Linn, M. Arnold
Multibody dynamics simulation of geometrically exact Cosserat rods
Keywords: flexible multibody dynamics, large deformations, finite rotations, constrained mechanical systems, structural dynamics
(20 pages, 2009)

160. P. Jung, S. Leyendecker, J. Linn, M. Ortiz
Discrete Lagrangian mechanics and geometrically exact Cosserat rods
Keywords: special Cosserat rods, Lagrangian mechanics, Noether's theorem, discrete mechanics, frame-indifference, holonomic constraints
(14 pages, 2009)

161. M. Burger, K. Dreßler, A. Marquardt, M. Speckert
Calculating invariant loads for system simulation in vehicle engineering
Keywords: iterative learning control, optimal control theory, differential algebraic equations(DAEs)
(18 pages, 2009)

162. M. Speckert, N. Ruf, K. Dreßler
Undesired drift of multibody models excited by measured accelerations or forces
Keywords: multibody simulation, full vehicle model, force-based simulation, drift due to noise
(19 pages, 2009)

163. A. Streit, K. Dreßler, M. Speckert, J. Lichter, T. Zenner, P. Bach
Anwendung statistischer Methoden zur Erstellung von Nutzungsprofilen für die Auslegung von Mobilbaggern
Keywords: Nutzungsvielfalt, Kundenbeanspruchung, Bemessungsgrundlagen
(13 pages, 2009)

164. I. Correia, S. Nickel, F. Saldanha-da-Gama
Anwendung statistischer Methoden zur Erstellung von Nutzungsprofilen für die Auslegung von Mobilbaggern
Keywords: Capacitated Hub Location, MIP formulations
(10 pages, 2009)

165. F. Yaneva, T. Grebe, A. Scherrer
An alternative view on global radiotherapy optimization problems
Keywords: radiotherapy planning, path-connected sublevelsets, modified gradient projection method, improving and feasible directions
(14 pages, 2009)

166 J. I. Serna, M. Monz, K.-H. Küfer, C. Thieke
Trade-off bounds and their effect in multi-criteria IMRT planning
Keywords: trade-off bounds, multi-criteria optimization, IMRT, Pareto surface
(15 pages, 2009)

167 W. Arne, N. Marheineke, A. Meister, R. Wegener
Numerical analysis of Cosserat rod and string models for viscous jets in rotational spinning processes
Keywords: Rotational spinning process, curved viscous fibers, asymptotic Cosserat models, boundary value problem, existence of numerical solutions
(18 pages, 2009)

Status quo: July 2009